2022-11

A multi-trophic marker approach reveals high feeding plasticity in Barents Sea under-ice fauna

Kohlbach, D

10.1016/j.pocean.2022.102895
Progress in Oceanography
Elsevier BV

Progress in Oceanography 208 (2022) 102895

Contents lists available at ScienceDirect

Progress in Oceanography

journal homepage: www.elsevier.com/locate/pocean

A multi-trophic marker approach reveals high feeding plasticity in Barents Sea under-ice fauna

Doreen Kohlbach [a,*], Lukas Smik [b], Simon T. Belt [b], Haakon Hop [a], Anette Wold [a], Martin Graeve [c], Philipp Assmy [a]

[a] Norwegian Polar Institute, Fram Centre, 9296 Tromsø, Norway
[b] School of Geography, Earth and Environmental Sciences, University of Plymouth, Plymouth, Devon PL4 8AA, United Kingdom
[c] Alfred Wegener Institute, Helmholtz Centre for Polar and Marine Research, 27570 Bremerhaven, Germany

A B S T R A C T

Microalgae growing within and attached to the bottom of Arctic sea ice (sympagic algae) can serve as a nutritious food resource for animals inhabiting the sea-ice water interface (under-ice fauna), particularly during the bottom ice-algal bloom in spring. As a consequence, under-ice fauna is likely impacted by sea-ice decline and changes in ice-algal primary production. To investigate this, samples of pelagic (=PPOM) and ice-associated particulate organic matter (=IPOM) and the ice-associated amphipods *Apherusa glacialis* and *Eusirus holmii*, and polar cod (*Boreogadus saida*), collected below ridged sea ice at two locations with pronounced differences in productivity in the northern Barents Sea during May 2021, were assessed for their trophic marker content. Specifically, we investigated the composition of diatom- and dinoflagellate-produced fatty acids (FAs), pelagic and sympagic highly branched isoprenoid (HBI) lipids as well as sterols to determine the animals' dietary preferences and trophic association to the sea-ice habitat during spring. Relative proportions of FAs differed strongly between PPOM and IPOM, indicating differences in species composition and degradation state between pelagic and sympagic habitats, respectively. FA signatures and sterol content of the consumers largely resembled known diet compositions with a strong reliance on diatom-derived carbon in *A. glacialis*, a higher degree of carnivory in *E. holmii* and evidence of *Calanus*-feeding in polar cod. Sympagic HBIs were detected at either low concentrations or not at all, in both producers and consumers, likely as a result of the very low abundance of their source diatoms. Pronounced trophic marker variability in *A. glacialis* collected at the highly productive shelf slope station versus the less productive central Arctic Basin station suggests a surprisingly high flexibility in carbon-source composition with a stronger reliance on pelagic food when available versus a higher importance of ice algal carbon when pelagic production is low. Nevertheless and despite the general lack (below detection limit) of sympagic HBIs in our dataset, high ice-algal biomass and elevated proportions of polyunsaturated FAs in IPOM compared to other seasons indicate that ice algae constitute a valuable nutritional carbon source as alternative to pelagic carbon during spring.

1. Introduction

Arctic sea ice represents a unique habitat for microscopic algae (Arrigo, 2017) and ice-algal biomass is often dominated by diatoms (Syvertsen, 1991; Ratkova and Wassmann, 2005; Lund-Hansen et al., 2017). Crustacea, such as copepods and amphipods (sympagic fauna), located within the sea-ice brine channels (ice meiofauna and some macrofauna) or dwelling at the sea ice-water interface (under-ice fauna; Hop et al., 2000; Gradinger et al., 2005; Werner, 2005; Arndt and Swadling, 2006; Bluhm et al., 2017) utilize sea-ice algae as a nutritional food source (Werner, 1997; Kohlbach et al., 2016; Brown et al., 2017) and channel it through the ice-associated food web (Ehrlich et al., 2021). Higher up the food chain, marine mammals rely on sea ice for foraging, resting, shelter and reproduction (Ainley et al., 2003; Laidre et al., 2015).

The Barents Sea seasonal ice-cover has been subject to change during all seasons over the past decades (Årthun et al., 2012; Onarheim and Årthun, 2017; Barton et al., 2018). Decline in sea-ice presence, extent and concentration (Kumar et al., 2021) alters timing, duration and magnitude of pelagic and sympagic primary production events (Dupont, 2012; Dalpadado et al., 2020; Song et al., 2021) with direct and indirect cascading impacts on food-web structures and trophic function in Arctic ecosystems (Kovacs et al., 2011; Barber et al., 2015; Stige et al., 2019; Pagano and Williams, 2021). Some marine animals have shown a positive response towards these alterations, as e.g. increasing biomass of capelin (*Mallotus villosus*) was linked to reduced sea-ice coverage in the

Abbreviations: CAO, Central Arctic Ocean; chl *a*, Chlorophyll *a*; FA, Fatty acids; HBI, Highly branched isoprenoid; IPOM, Ice-associated particulate organic matter; PPOM, Pelagic particulate organic matter; PUFA, Polyunsaturated fatty acid.

* Corresponding author.
E-mail addresses: doreen.kohlbach@npolar.no (D. Kohlbach), lukas.smik@plymouth.ac.uk, lukas.smik@gmail.com (L. Smik), s.belt@plymouth.ac.uk (S.T. Belt), haakon.hop@npolar.no (H. Hop), anette.wold@npolar.no (A. Wold), martin.graeve@awi.de (M. Graeve), philipp.assmy@npolar.no (P. Assmy).

https://doi.org/10.1016/j.pocean.2022.102895
Received 19 March 2022; Received in revised form 8 July 2022; Accepted 6 September 2022
Available online 14 September 2022

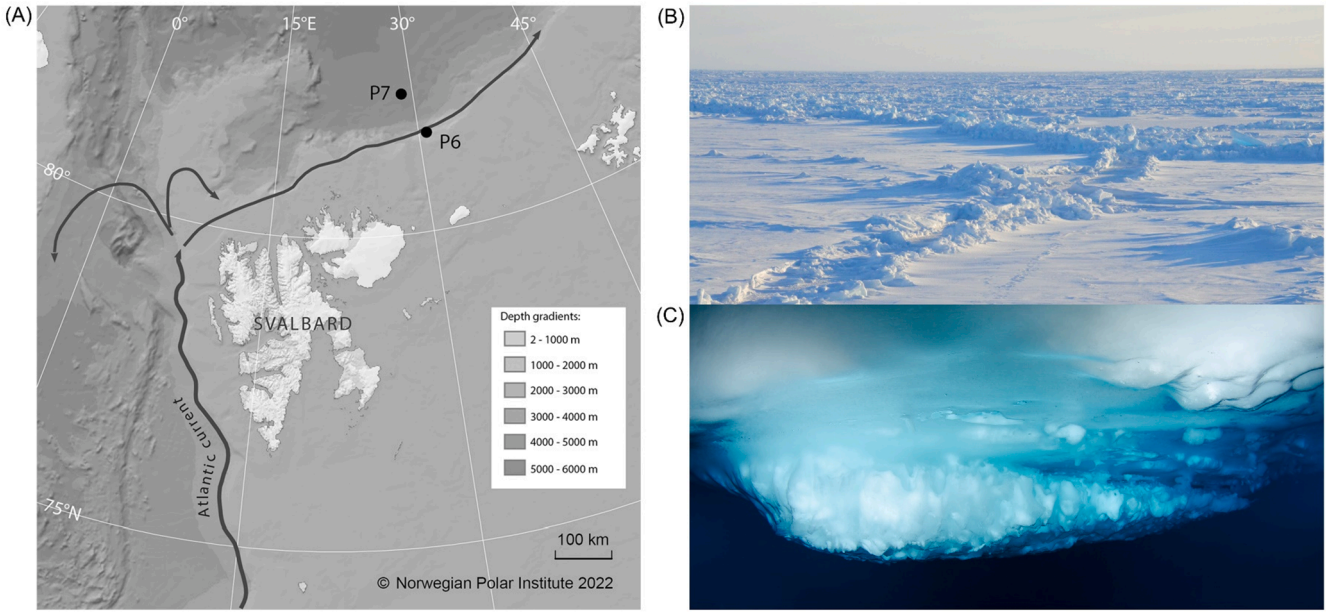

Fig. 1. (A) Sampling stations P6 and P7 in the northern Barents Sea, visited in May 2021, (B) Sea-ice ridge top, (C) Sea-ice ridge bottom. Photos: Haakon Hop (B) and Peter Leopold (C; from N-ICE2015 expedition).

Barents Sea (Stige et al., 2019). However, a strong dependency on the sea-ice habitat can leave some species highly vulnerable towards these changes, e.g. regarding their reproductive cycle and consequently success of offspring, body condition and subsequently abundance/biomass of organisms across all trophic levels (Wassmann et al., 2011; Hop et al., 2019, 2021; Møller and Nielsen, 2020). Moreover, northward expansion of Atlantic water masses (so-called Atlantification; Asbjørnsen et al., 2020; Ingvaldsen et al., 2021) can cause species re-distribution with a poleward range expansion of boreal species (Dalpadado et al., 2012; Eriksen et al., 2017; Aarflot et al., 2018; Ershova et al., 2021).

In the Arctic, the gammaridean amphipod *Apherusa glacialis* is one of the dominant sea ice-associated species (Hop et al., 2000, 2021; Poltermann, 2001). Such herbivorous sympagic amphipods link the base of the Arctic marine food-web to intermediate and higher trophic levels (Lønne and Gulliksen, 1989; Lønne and Gabrielsen, 1992; Jakubas et al., 2011; Ogloff et al., 2020) and couple sympagic with pelagic and benthic food-web processes (Scott et al., 1999; Kohlbach et al., 2016). *Apherusa glacialis* is typically regarded to spend all or most of its lifecycle associated with sea ice (autochthonous) (Lønne and Gulliksen, 1991; Beuchel and Lønne, 2002). Recent investigations, however, challenge this assumption and indicate that *A. glacialis* can also occur throughout the water column, irrespective of the season (Kunisch et al., 2020), which could ultimately make this species less vulnerable and more adaptable to continued sea-ice retreat than previously assumed (Berge et al., 2012; Drivdal et al., 2021). In the case of the predatory gammaridean amphipod *Eusirus holmii*, the strength and nature of the ice association is less clear (Macnaughton et al., 2007) and it seems to be less reliant on sympagic carbon than *A. glacialis* (Brown et al., 2017). However, *E. holmii* is frequently found in close proximity to the ice (Gradinger et al., 2010; David et al., 2015; Hop et al., 2021) and has been shown to utilize ice algae as an energy source (Kohlbach et al., 2016).

Apherusa glacialis can serve as an important food item in the diet of polar cod (*Boreogadus saida)* (Lønne and Gulliksen, 1989; Kohlbach et al., 2017), a key species for the energy transfer within the Arctic food-web, which in turn is preyed on by many species of seals, whales and seabirds (Bradstreet and Cross, 1982; Hop and Gjøsæter, 2013). Although polar cod usually spends only part of its life cycle closely associated with the ice (Lønne and Gulliksen, 1989; Gradinger and Bluhm, 2004; David et al., 2016), it might be particularly sensitive to sea-ice loss (Huserbråten et al., 2019) due to its reliance on the ice for spawning and the development of the larvae in the under-ice environment (Eriksen et al., 2015; Dahlke et al., 2018; Gjøsæter et al., 2020). Other findings, however, suggest that reduced sea ice might have a positive effect on the growth of this species since low sea-ice concentration during winter potentially extends the period of suitable growth conditions (Dupont et al., 2020).

Based on the analysis of compound-specific stable isotopes, Kohlbach et al. (2016) concluded that up to 92 % of the dietary carbon of *A. glacialis* from the central Arctic Ocean (CAO) was sourced from ice algae during summer, and that the sea-ice signal was transferred to young polar cod inhabiting the under-ice environment, preying extensively on these amphipods (Kohlbach et al., 2017). Using the presence of sympagic highly branched isoprenoid (HBI) lipids (Brown and Belt, 2012; Brown et al., 2014; Belt, 2018), an approach also applied in this study (details in Schmidt et al., 2018; Kohlbach et al., 2021a), the importance of ice algae as a carbon source for *A. glacialis* was similarly high in individuals collected in Svalbard waters during summer (Brown et al., 2017). A somewhat lower contribution (up to 79 %) from sea-ice algae was found for the carbon budget of *Eusirus holmii* in the CAO during summer (based on the stable isotope method; Kohlbach et al., 2016), while Brown et al. (2017) identified a relatively low ice algae carbon content for this species sampled in the Nansen Basin, implying that it obtained the majority of its organic carbon from other sources.

Besides these previous results, information on carbon sources utilized by under-ice fauna using trophic marker approaches is relatively scarce (e.g., Budge et al., 2008), emphasizing the need for more data collection from different regions of the Arctic Ocean as well as from different seasons, especially as dietary requirements of marine animals can underlie seasonal trends (Kohlbach et al., 2021b). Changes at these lower trophic levels can have important implications for the entire carbon flow as well as carbon cycling (Ehrlich et al., 2021). As a region of extreme environmental change, the Barents Sea offers the opportunity to closely study the effects of climate change on marine life (e.g. Dalpadado et al., 2020; Koenigstein, 2020; Ingvaldsen et al., 2021). Sea-ice ridges have been suggested as ecological hotspots that host a particularly rich biodiversity and suitable habitat for sea ice-associated flora and fauna (Hop et al., 2000; Gradinger et al., 2010; Lange et al., 2017; Fernández-Méndez et al., 2018), but are likely to be altered in structure and distribution under increasing temperatures and wind (Wadhams and Toberg, 2012).

Table 1
Sampling information for pelagic and ice-associated particulate organic matter (POM) and under-ice fauna collected during Nansen Legacy cruise Q2 in April/May 2021 in the Barents Sea.

Station #	Date of sampling (2021)	Latitude °N	Longitude °E	Sea-ice thickness (cm)[a]	Snow depth (cm)[b]	Sea-ice freeboard (cm)[a]	Bottom depth (m)	Sampling gear	Sample type
P6	09/05	81.562	30.746	109 ± 9	14 ± 2	6 ± 3	1113	CTD	Pelagic POM
	10/05	81.563	30.829				1407	Slurp gun	Ice-associated POM
	11/05	81.473	29.553				297	Suction pump	Ice amphipods
								Spear	Polar cod
P7	13/05	82.147	29.139	138 ± 2	5 ± 1	10 ± 1	3509	CTD	Pelagic POM
		82.227	28.696				3197	Slurp gun	Ice-associated POM
		82.227	28.696					Suction pump	Ice amphipods

[a] $n = 6$ per station.
[b] at location of ice-core sampling, $n = 3$ for each core, total $n = 18$.

To study carbon and food source compositions of marine organisms, a suite of biochemical methods can be used, including the analysis of fatty acids (FAs), HBIs and sterols, preferably applied as a multi-trophic marker approach (discussed in Kohlbach et al., 2021a and references there). Here, we investigated the FA composition of typical Arctic under-ice fauna species (*A. glacialis*, *E. holmii*, polar cod) collected in the (northern) Barents Sea to assess their dietary requirements (see Dalsgaard et al., 2003) during May 2021, when ice algae were expected to represent a nutritious food source. Furthermore, we traced the sea-ice signal from producers to consumers using the presence/absence of sympagic HBIs (*i.e.*, IP_{25} and $IPSO_{25}$; e.g. Kohlbach et al., 2019; Yunda-Guarin et al., 2020). Sterols reflected the importance of heterotrophic food items in the diet of the investigated species (Ruess and Müller-Navarra, 2019). The results contribute to our understanding of the importance of sea ice-derived food sources for the ice-associated food web under current sea-ice conditions.

2. Material and methods

2.1. Sampling

As part of the Norwegian Nansen Legacy project (arvenetternansen.com; Wassmann, 2022), samples of pelagic particulate organic matter (PPOM), ice-associated POM (IPOM) and typical representatives of the Arctic under-ice fauna were collected during the Nansen Legacy seasonal cruise Q2 (27 April to 20 May 2021) with RV *Kronprins Haakon* in the northern Barents Sea. Samples for this study were taken between 9 and 13 May 2021 at the ice-covered sampling stations P6 and P7 (Fig. 1**A**, Table 1). The sea ice encountered during our sampling campaign was ridged at both sampling stations (Fig. 1**B, C**).

PPOM was collected at 20 m depth with Niskin bottles attached to a CTD rosette. IPOM was sampled in sea-ice ridges by divers with a slurp gun at both stations (Fig. 2**A, B**). Both seawater (between 2.5 and 3 L) and IPOM samples (50 mL) were filtered through pre-combusted (3 h, 550 °C) 47 mm Whatman® GF/F filters. Filters were frozen at −80 °C until further processing.

The under-ice sampling of ice fauna was facilitated by divers with varying equipment (Fig. 2**C, D**). The under-ice amphipods *Apherusa glacialis* and *Eusirus holmii* were collected with a suction pump at both stations (Fig. 2**C**, Table 2). Small individuals of *A. glacialis* (<10 mm) were pooled to obtain sufficient material for subsequent analyses (between 5 and 9 individuals per sample) and up to three individuals of *E. holmii* were pooled. Polar cod were caught with a spear (Fig. 2**D**) and immediately dissected to retrieve muscle and liver tissue for analyses. All samples were frozen at −80 °C.

Chlorophyll (chl) *a* was sampled at 20 m with a CTD rosette, for the bottom 10 cm of level sea ice with a 9 cm diameter Kovacs ice corer and at ridge surfaces by divers with a slurp gun (Fig. 2**B**). All samples were filtered through 25 mm Whatman® GF/F filters under low vacuum pressure (~30 kPa). Filters were stored in polypropylene tubes with 5 mL of methanol added for extraction (overnight at 0–4 °C). Chlorophyll *a* concentrations were measured on a Trilogy Laboratory fluorometer (Turner Designs, CA, USA) before and after acidification with two drops of 5 % HCl according to Holm-Hansen and Riemann (1978).

2.2. Fatty acids (FAs)

FA compositions of POM and animals were analysed at Akvaplan-niva, Tromsø, Norway. Lipids were extracted after Folch et al. (1957) with methanol/dichloromethane (1:2). FAs were transesterified to fatty acid methyl esters (FAMEs) with 1 % sulfuric acid in methanol at 50 °C for 16 h and extracted with hexane/ether (1:1, v/v). FAMEs were analysed on an Agilent 7890 gas chromatograph with a capillary glass column (Agilent/Varian CP7419 Select FAME; 50 m × 0.25 mm ID × 0.25 μm film thickness), equipped with a flame ionization detector (FID) using a temperature program (60 °C, 1 min → 30 °C/min → 130 °C, 0 min → 1.3 °C/min → 195 °C, 0 min → 30 °C/min → 230 °C, 3 min). Samples were injected split-less and hydrogen was used as a carrier gas. FAMEs were identified via reference standard mixtures (GLC96 and GLC68D from NuCheck-Prep) containing known amounts of the relevant compounds. FAs were quantified with an internal standard (21:0) that was added prior to lipid extraction, using individual FA response factors determined from the standard solutions. The proportions of individual FAs were expressed as mass percentage of the total FA content as well as concentrations (g 100 g $lipid^{-1}$; Table A.1). Sample size for each sample type/species can be found in Table 4.

We assessed proportional contributions and ratios of FAs that can provide dietary information on carbon source preferences of the consumers (trophic marker FAs): the FAs 16:1(n-7), 16:4(n-1) and 20:5(n-3) are produced by diatoms (*i.e.*, diatom-associated FAs), and the FAs 18:4 (n-3) and 22:6(n-3) (*i.e.*, dinoflagellate-associated FAs) are predominantly produced by dinoflagellates and the prymnesiophyte *Phaeocystis* (Falk-Petersen et al., 1998; Reuss and Poulsen, 2002; Dalsgaard et al., 2003). Long-chained FAs 20:1 and 22:1 (all isomers) were used to indicate the reliance of the predatory species on copepods, such as *Calanus* spp. (Falk-Petersen et al., 1990; Søreide et al., 2013). Polyunsaturated FAs (PUFAs), such as 20:5(n-3) and 22:6(n-3), are incorporated into membrane (polar) lipids for stabilization, while 16:1(n-7) and the copepod-associated FAs are predominantly incorporated into storage (neutral) lipids (Stübing et al., 2003; Taipale et al., 2011).

2.3. Highly branched isoprenoids (HBIs) and sterols

HBIs and sterols were analysed at the University of Plymouth, UK (polar cod: only muscle tissue was analysed). Detailed information on analytical procedure and equipment is given in Kohlbach et al. (2021a).

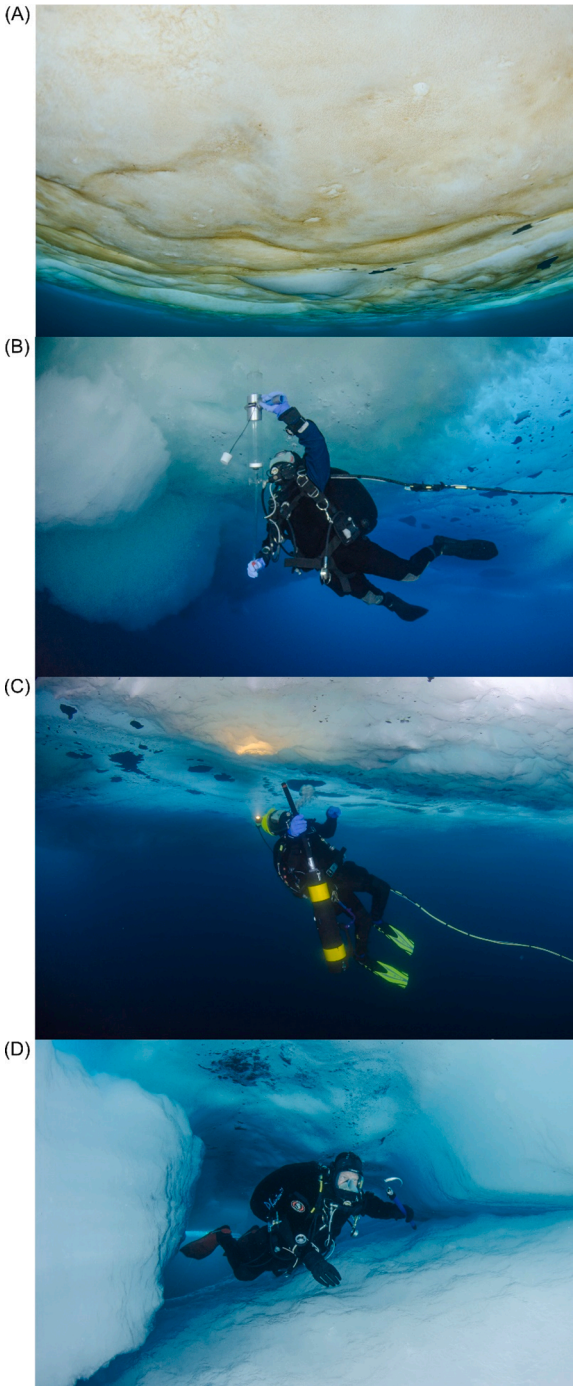

Fig. 2. (A) Sea-ice algae growing at the bottom of level ice, picture taken 7 May 2021, 79.68 °N, 33.53 °E; Sampling of (B) IPOM with a slurp gun (scientific diver Amalia Keck Al-Habahbeh), (C) under-ice amphipods with a suction pump (scientific diver: Haakon Hop), and (D) polar cod with a spear within a sea-ice ridge (scientific diver Mikko Vihtakari). Photos: Peter Leopold.

Briefly, samples were freeze-dried and homogenized. Thereafter, samples were saponified (70 °C; 60 min) with 20 % potassium hydroxide in water/methanol (1:9, v/v). Non-saponifiable lipids were extracted with hexane and purified by open column chromatography (silica gel, 60–200 μm, ca. 0.5 g).

HBIs were eluted with hexane (five column volumes) before being dried under gentle N_2 stream (25 °C) and analysed by gas chromatography-mass spectrometry (GC–MS). The analysis was carried out on an Agilent 7890A gas chromatograph (GC), coupled to an Agilent

Table 2
Dimensions of species analysed in this study (mean ± 1 SD, range is given in brackets).

Species	Station	Total length (mm)	*n*	Weight	Tissue analysed
Apherusa glacialis Hansen, 1887	P6, P7	<10	20 22	10.5 ± 3.4 mg (4.6 – 16.3 mg)[a] 1.7 ± 0.3 mg (1.0 – 2.2 mg)[b]	Entire animal
Eusirus holmii Hansen, 1887	P7	<10, 30, 40	4 3	197.8 ± 244.9 mg (11.4 – 528 mg)[a] 15.1 ± 19.2 mg (2.9 – 37.2 mg)[b]	Entire animal
Boreogadus saida Lepechin, 1774	P6	118 ± 13	4	11.4 ± 2.5 g (9.4 – 14.2 g)[c]	Muscle, liver

[a] wet weight per individual for FA analysis.
[b] dry weight per individual for HBI analysis.
[c] wet weight entire fish.

5975 Mass Selective Detector (MSD), fitted with an Agilent HP-5 ms column (30 m length × 0.25 mm internal diameter × 0.25 μm film thickness) with auto-splitless injection (300 °C) and helium carrier gas (1 mL min^{-1} constant flow). Analysis was carried out by total ion current (TIC; *m/z* 50–500) and selective ion monitoring (SIM) techniques (70 eV) using a ramped temperature programme of 10 °C min^{-1} from 40 to 300 °C followed by a 10 min isothermal at 300 °C. Identification of HBIs was achieved following analysis in selective ion monitoring (SIM; *m/z* 350.3 [IP_{25}], *m/z* 348.3 [$IPSO_{25}$] and *m/z* 346.3 [HBIs III and IV]; limit of detection = 10 ng mL^{-1}) by comparing relative retention times with those of purified standards. Quantification of HBIs was achieved by integrating individual ion responses in SIM mode and normalising these to the corresponding peak area of the internal standard (9-octyl-8-heptadecene (9-OHD): *m/z* 350.3) and an instrumental response factor obtained from purified standards (Belt et al., 2012). The two tri-unsaturated HBIs (HBIs III and IV) were used to assess the consumption of pelagic algal material, including that from the marginal ice zone (MIZ) (Brown et al., 2014; Belt, 2018). The mono- and di-unsaturated HBIs IP_{25} and $IPSO_{25}$, assumed to be produced exclusively by certain sea-ice diatoms, were assessed to provide information about the reliance of the consumers on sympagic carbon (Brown et al., 2018; Schmidt et al., 2018).

Furthermore, we analysed the phytoplankton-produced sterols (hereafter referred to as phytosterols) brassicasterol (24-methylcholesta-5,22E-dien-3β–ol; *m/z* 470), sitosterol (24-ethylcholest-5-en-3β–ol; *m/z* 396), chalinasterol (24-methylcholesta-5,24(28)-dien-3β–ol; *m/z* 470) and campesterol (24-methylcholest-5-en-3β–ol; *m/z* 382) and the phyto-and-zooplankton-produced sterols (hereafter referred to as zoosterols) cholesterol (Cholest-5-en-3β–ol; *m/z* 458), desmosterol (Cholesta-5,24-dien-3β–ol; *m/z* 343) and dehydrocholesterol (Cholesta-5,22E-dien-3β–ol; *m/z* 327).

Sterols were eluted from the silica column using hexane:methylacetate (4:1,v/v), dried (N_2) and derivatised using N,O-bis (trimethylsilyl)trifluoroacetamide (BSTFA; 70 °C, 1 h) prior to analysis by GC–MS. Individual sterols were identified by comparison of the mass spectra of their trimethylsilylethers with published data (Belt et al., 2018). Quantification of individual sterols was carried out in the SIM mode utilising 5α-androstan-3β-ol (*m/z* 333) as an internal standard.

The GC–MS-derived masses of HBIs and sterols were converted to water column/sea-ice concentrations using the volume of filtered sea water (2.5–3 L) and sea ice (50 mL), respectively, and to concentrations in zooplankton body using the mass of the sample extracted (8–100 mg).

Sample size was $n = 3$ for PPOM, $n = 10$ for IPOM, $n = 14$ for *A. glacialis*, $n = 3$ for *E. holmii* and $n = 4$ for polar cod.

Table 3
Chlorophyll *a* concentrations (A. Vader et al., dataset submitted for publication) at 20 m depth and in sea ice at the two sampling locations.

Chlorophyll *a* (mg m^{-3})	*n*	Station P6: shelf slope	*n*	Station P7: deep Arctic Basin
Seawater 20 m	1	3.7	1	0.3
Ice core, level ice bottom 0–3 cm[a]	1	10.7	1	15.4
Under-ice, ridge bottom	3	5.1 ± 1.4	3	2.2 ± 0.4
Under-ice, ridge side	2	1.2 ± 0.1	3	1.6 ± 0.02
Under ice, ridge overhead	1	15.2	3	1.6 ± 0.3

[a] based on three pooled ice-core bottoms.

2.4. Data analysis

Variability in FA datasets of POM and the under-ice fauna species was visualized with correspondence analysis (CA), suitable for analysing compositional data (Greenacre and Primicerio, 2014; Greenacre, 2017). Differences of FA proportions between the two sampling stations in PPOM, IPOM and *A. glacialis* were assessed using Wilcoxon rank sum tests; 1-way ANOVAs followed by Tukey's HSD post-hoc tests were applied when assessing seasonal differences of FA proportions in PPOM and IPOM. A statistical threshold of $\alpha = 0.05$ was chosen, and results with $p \leq 0.05$ were considered significant. Prior to statistical analysis, the data were verified for normality of distribution. All measures of statistical variation are reported as means ± 1 SD. All statistical analyses and data visualization were done in R v.4.1.0 (R Core Team, 2021) using the packages 'ggplot2' (Wickham, 2016) and 'vegan' (Oksanen et al., 2020).

3. Results & discussion

The under-ice biota sampled by the divers was strongly dominated by *Apherusa glacialis*, which is in line with its pan-Arctic occurrence and importance as part of the sympagic fauna in Arctic ecosystems (David et al., 2015; Ehrlich et al., 2020; Hop et al., 2021). *Eusirus holmii* has been described as a hyperbenthic species, restricted to water masses with temperatures lower than 1 °C (Weisshappel, 2000), but with a wide depth range from 400 to 1600 m (Lörz et al., 2018). *Eusirus holmii* is, however, also well known to be associated with the sea-ice habitat (Tencati and Geiger, 1968) and has been identified as part of the under-ice fauna in the CAO (David et al., 2015) and the waters north of Svalbard (Ehrlich et al., 2020). *Eusirus holmii* is typically less abundant in the ice-fauna community than *A. glacialis* (Brown et al., 2017; Ehrlich et al., 2020), which was also the case in this study. Juvenile polar cod *Boreogadus saida* has frequently been described to inhabit the under-ice environment (Gradinger and Bluhm, 2004; Melnikov and Chernova, 2013; David et al., 2016; Huserbråten et al., 2019). Although generally abundant in the northern Barents Sea (Hop and Gjøsæter, 2013; McBride et al., 2014), in this study, the divers collected only four individuals at station P6. If present, polar cod are generally hiding within ridges, in open spaces as present at P6 (but not at P7). With many demands for sampling by divers, polar cod were only searched for and caught in a few dives during the expedition.

3.1. Pelagic and ice-associated particulate organic matter

Despite their close proximity, the two sampling stations reflected different water mass regimes (Fig. 1**A**): P6 was more representative of the highly productive shelf-regime, while P7 was more representative of the low-productive central Arctic Basin. An under-ice phytoplankton bloom occurred at station P6, which was dominated by pelagic diatoms of the genus *Thalassiosira* (P. Assmy, pers. obs., and congruent with the literature: Moran et al., 2012), while the chl *a* concentrations in the water column at P7 were lower by one order of magnitude (Table 3). Chlorophyll *a* concentrations > 10 mg m^{-3} in the bottom three cm of level sea ice at both stations (Table 3) indicated that the vernal ice algal bloom was in full progress during our sampling. Chlorophyll *a* concentrations in the bottom sections of level ice at the same sampling locations were distinctly lower during (late) summer (≤2.3 mg m^{-3}) and (early) winter (≤0.3 mg m^{-3}) (Vader et al., 2021), emphasizing seasonal variations in ice-algal productivity (Leu et al., 2011; Ji et al., 2013). The ridge at P7 was more consolidated (H. Hop, pers. obs.) and had fewer open spaces and less surface area compared to the ridge at P6, which

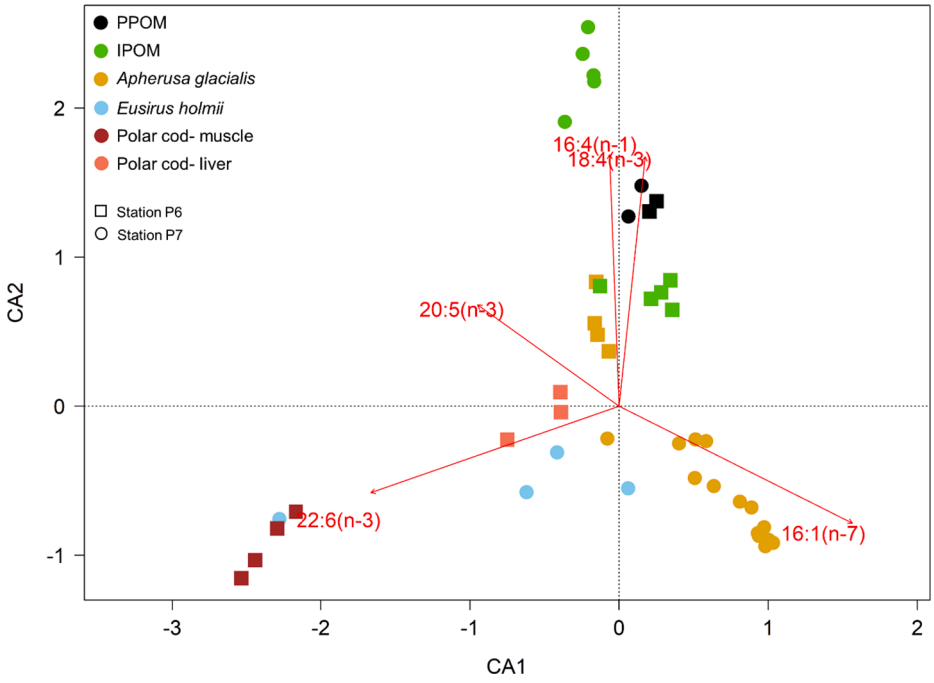

Fig. 3. Correspondence analysis (CA) of the relative proportions of the trophic marker fatty acids 16:1(n-7), 16:4(n-1) and 20:5(n-3) (diatom-associated), 18:4(n-3) and 22:6(n-3) (dinoflagellate-associated) in pelagic particulate organic matter (PPOM), ice-associated POM (IPOM) and the under-ice fauna. Datapoints represent individual samples.

Table 4
Relative proportions (mean ± 1 SD %) of the most abundant fatty acids in pelagic particulate organic matter (PPOM), ice-associated POM (IPOM) and under-ice fauna. Concentrations (mean ± 1 SD g 100 g lipid^{-1}) are given in Table A.1.

Fatty acids	PPOM	IPOM	*Apherusa glacialis*	*Eusirus holmii*	Polar cod-muscle	Polar cod-liver
n	4 (P6: 2, P7: 2)	10 (P6: 5, P7: 5)	20 (P6: 4, P7: 16)	4 (all P7)	4 (all P6)	3 (all P6)
14:0	8.4 ± 0.5	10.1 ± 0.7	2.9 ± 0.4	2.3 ± 1.3	2.4 ± 0.8	5.1 ± 1.0
16:0	19.4 ± 7.6	20.7 ± 1.2	13.8 ± 0.9	12.4 ± 0.9	16.3 ± 1.1	8.2 ± 0.2
16:1(n-7)[a]	12.0 ± 2.9	17.6 ± 6.8	38.2 ± 9.6	15.2 ± 9.6	2.8 ± 0.7	10.3 ± 0.5
16:4(n-1)[a]	2.0 ± 1.4	3.4 ± 0.8	1.0 ± 0.7	0.3 ± 0.4	0.1 ± 0.001	0.2 ± 0.02
18:0	6.3 ± 1.6	2.7 ± 1.3	0.9 ± 0.2	0.9 ± 0.2	2.5 ± 0.6	1.1 ± 0.1
18:1(n-9)	7.3 ± 2.5	3.3 ± 1.6	14.1 ± 1.5	15.7 ± 0.8	5.5 ± 0.6	5.2 ± 0.6
18:4(n-3)[b]	3.0 ± 0.5	3.1 ± 0.5	0.9 ± 0.4	0.5 ± 0.3	0.9 ± 0.2	1.6 ± 0.3
Σ20:1[c]	5.9 ± 6.0	1.7 ± 0.8	1.4 ± 0.6	9.2 ± 5.5	6.9 ± 1.9	24.7 ± 0.5
20:5(n-3)[a]	5.6 ± 0.8	16.2 ± 2.7	13.0 ± 5.1	14.0 ± 4.9	16.7 ± 0.2	7.4 ± 1.1
Σ22:1[c]	7.4 ± 7.5	1.6 ± 0.7	0.6 ± 0.3	4.9 ± 3.5	3.9 ± 1.8	19.9 ± 0.7
22:6(n-3)[b]	2.9 ± 0.6	4.4 ± 1.2	4.9 ± 2.2	14.9 ± 10.3	32.5 ± 4.7	6.8 ± 1.6
16:1(n-7)/16:0[d]	0.7 ± 0.1	0.9 ± 0.4	2.8 ± 0.7	1.2 ± 0.8	0.2 ± 0.1	1.3 ± 0.1
ΣC16/ΣC18[d]	1.6 ± 0.6	4.3 ± 1.7	2.6 ± 0.4	1.3 ± 0.4	1.6 ± 0.2	1.7 ± 0.1
20:5(n-3)/22:6(n-3)[d]	2.0 ± 0.3	3.9 ± 1.2	2.8 ± 0.4	1.1 ± 0.3	0.5 ± 0.1	1.1 ± 0.1
ΣPUFAs[e]	23.9 ± 3.3	34.3 ± 4.2	24.1 ± 9.1	34.2 ± 14.9	54.2 ± 4.7	20.3 ± 2.8

[a] diatom-associated FA.
[b] dinoflagellate-associated FA.
[c] copepod-associated FA: isomers 20:1 and 22:1 are synthesized *de novo* by *Calanus* spp.; they typically indicate the importance of *Calanus* spp. and other copepods as a food source for a consumer (Sargent and Falk-Petersen, 1988; Falk-Petersen et al., 1990).
[d] Ratios of 16:1(n-7)/16:0, the sum of C16 FAs (produced in high amounts by diatoms) versus the sum of C18 FAs (produced in high amounts by dinoflagellates; hereafter referred to as ΣC16/ΣC18), and the FA ratio 20:5(n-3)/22:6(n-3) > 1 can indicate a dominance of diatom-produced versus dinoflagellate-produced carbon.
[e] Relative proportions of polyunsaturated FAs (PUFAs) can be used as an indicator of food quality of an algal community (Søreide et al., 2010).

might explain the somewhat lower chl *a* biomass in the different ridge surfaces sampled at P7.

Fatty acid (FA) profiles of PPOM and IPOM differed substantially (Fig. 3, Table 4) and also between the two sampling locations (Fig. 4), pointing, on the one hand, to differences in algal community composition and on the other hand, to differences in physiological state of the algal communities and bloom succession (Falk-Petersen et al., 1998; Wang et al., 2014). Consistent with some previous studies (McMahon et al., 2006; Kohlbach et al., 2021a), the diatom signal was overall stronger in IPOM than in PPOM; however, dinoflagellates contributed to both pelagic and sympagic algal communities in low quantities (Table 4).

In PPOM, the diatom-associated FAs 16:1(n-7) and 16:4(n-1) had higher average contributions to the FA profile at station P6 compared to P7, while the dinoflagellate signal was similar at both stations, which is in agreement with the dominance of pelagic diatoms at P6 (Fig. 4**A**). Concentrations of the diatom-associated FA 20:5(n-3) in PPOM were similar between the stations. IPOM collected at station P6 had, on average, twice as much 16:1(n-7) compared to P7, whereas the other two diatom-associated FAs 16:4(n-1) and 20:5(n-3) had significantly higher contributions at station P7 compared to P6 (Fig. 4**B**). As seen for PPOM, contributions of both dinoflagellate-associated FAs (18:4(n-3) and 22:6(n-3)) were more similar between the two sampling locations than diatom-associated FAs (Fig. 4**B**), indicating that diatoms were the main drivers of variability.

Polar lipids used for the stabilization of bio-membranes have a high contribution of polyunsaturated FAs (PUFAs), such as 20:5(n-3) and 22:6(n-3) (Lee et al., 2006), which are essential for successful growth and reproduction of Arctic animals (Sargent, 1995; Brett and Müller-Navarra, 1997). Concentrations are highest in the beginning of the bloom (Falk-Petersen et al., 1998), translating into a high food quality for the dependent food web (Gulati and Demott, 1997; Søreide et al., 2010), with a gradual shift to a dominance of neutral lipids for energy storage towards the end of the bloom (Smith et al., 1993). In accordance with the literature and the seasonal progression of blooming events, in the current study, IPOM had the highest PUFA production in spring and lowest nutritional value during advanced summer ice melt (Kohlbach et al., 2021a), while PUFA production by pelagic algae peaked during summer (Fig. 5). It has to be considered, however, that the FA content is not only a function of time, but also strongly dependent on the dominating algae species (Henderson et al., 1998).

At P6, IPOM collected by the divers contained all HBIs analysed for, of both pelagic (HBIs III and IV) and sympagic (IP_{25} and $IPSO_{25}$) origin (Fig. 6**A**). In all P6 IPOM samples, the concentrations of pelagic HBIs were approx. ten times higher (sum up to 3272 pg mL^{-1}) than sympagic HBIs (sum up to 315 pg mL^{-1}). HBI III (1546 to 2413 pg mL^{-1}) was approx. three times more concentrated than HBI IV (571 to 859 pg mL^{-1}), while $IPSO_{25}$ concentrations (208 to 279 pg mL^{-1}) were roughly one magnitude higher compared to IP_{25} concentrations (26 to 36 pg mL^{-1}). The presence of pelagic HBIs in IPOM is likely a consequence of the sampling technique and the under-ice bloom at P6 during the time of sampling. The divers collected bottom-ice algal material with slurp guns, which also sucked in some of the surrounding seawater at the ice-water interface, a suggestion supported by microscopic identification of pelagic diatoms such as *Thalassiosira* spp. in some slurp gun samples (P. Assmy, unpubl. data). In contrast, no HBIs were detected in IPOM at P7. The sympagic HBI-producing algal taxa (*Haslea crucigeroides, H. spicula, H. kjellmanii* and *Pleurosigma stuxbergii* var *rhomboides*) are generally not among the dominant taxa in Arctic ice-algal communities (von Quillfeldt, 2000; Brown et al., 2014). In our study, *Haslea* spp. were not detected in taxonomic investigations of slurp gun samples, while *Pleurosigma* sp. occurred at very low abundances (P. Assmy, unpubl. data). Thus, the absence of HBIs in IPOM from P7 was likely the result of the lower algal biomass and thus lower contribution of HBI-producing algae. Moreover, the ridge at P6 was younger with a more complex surface area and thus potentially with more algal patches than the older more consolidated ridge at P7 (H. Hop, pers. obs.). No HBIs were detected in the bottom 3 cm of ice cores collected with a 9 cm ice corer (Kovacs) at both stations ($n = 4$), with the exception of IP_{25} at low concentration in one ice core from station P7 (4.6 pg mL^{-1}). These differences in HBI content between material collected by divers and those collected with an ice corer might reflect differences in mode of collection. The distribution of ice algae is known to be heterogeneous (Rysgaard et al., 2001; Lange et al., 2016), leading to potentially high variability in sample material collected 'blindly' with ice corers. In contrast, divers targeted under-ice areas with visibly high levels of biomass, increasing the probability of collecting HBI-producing algae in higher concentrations. Another explanation could be the loss of bottom-ice algal material during the ice core retrieval.

Concentrations of phytosterols and zoosterols were positively correlated in the POM samples (Fig. 6**B**; Pearson's correlation: corr.

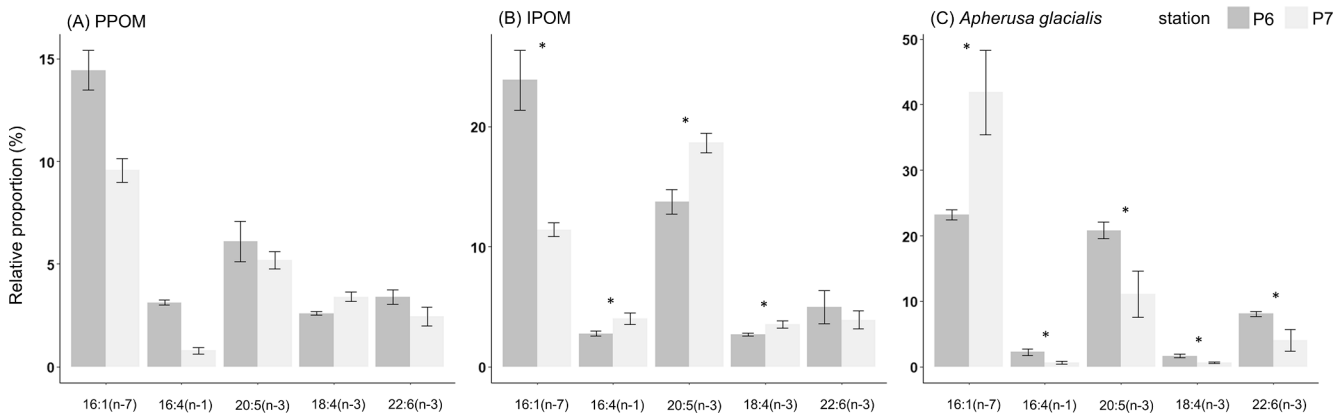

Fig. 4. Differences in the relative proportions (mean ± 1 SD %) of the trophic marker fatty acids 16:1(n-7), 16:4(n-1) and 20:5(n-3) (diatom-associated), 18:4(n-3) and 22:6(n-3) (dinoflagellate-associated) in (A) pelagic particulate organic matter (PPOM), (B) ice-associated POM (IPOM) and (C) the amphipod *Apherusa glacialis* at stations P6 and P7. Associated bars marked with asterisk "*" represent significant differences between the stations (Wilcoxon test $p < 0.05$).

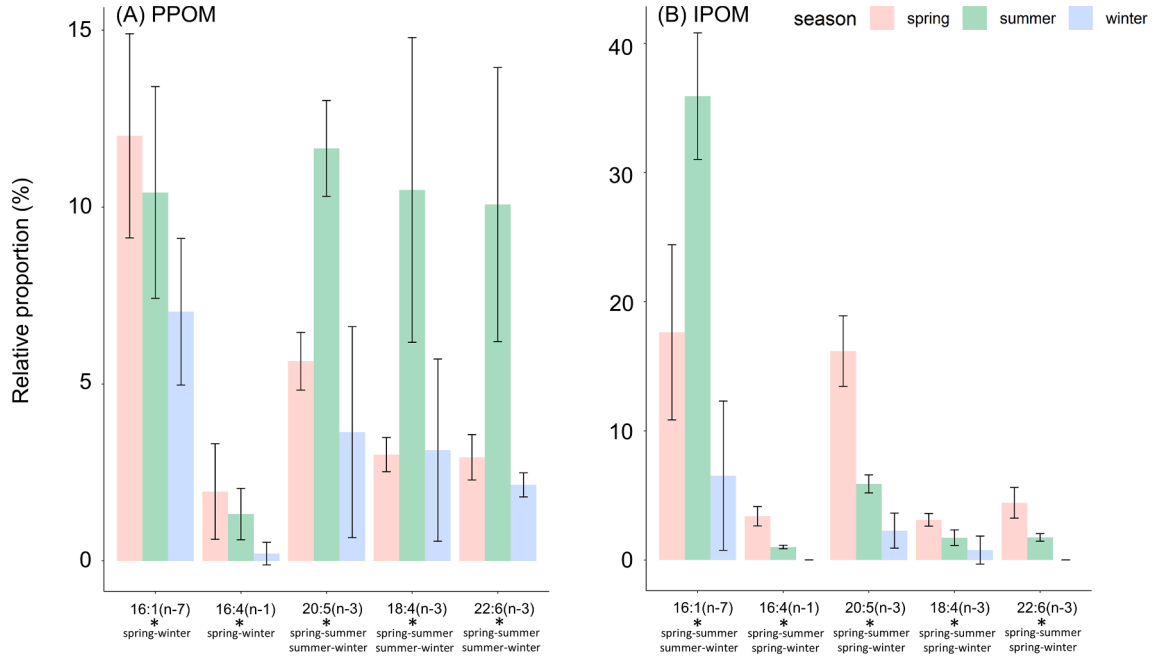

Fig. 5. Seasonal differences in the relative proportions (mean ± 1 SD %) of the trophic marker fatty acids 16:1(n-7), 16:4(n-1) and 20:5(n-3) (diatom-associated), 18:4(n-3) and 22:6(n-3) (dinoflagellate-associated) in (A) pelagic particulate organic matter (PPOM) and (B) ice-associated POM (IPOM). Dates of sampling: spring- this study, summer- 5 to 27 August 2019, winter- 28 November to 17 December 2019. I-POM samples from summer and winter were collected via ice coring (details on sampling and stations: Kohlbach et al., 2021a, b). Considered are only samples collected at stations *P*6 and P7 in all seasons (exception: winter IPOM sampling at station P5 instead of *P*6; see Kohlbach et al., 2021b for map). Note: different scales. Asterisk "*" represents significant differences between the seasons listed below (ANOVA test $p < 0.05$).

coeff. = 0.97, $p < 0.001$). The ratios of zoosterols/phytosterols were somewhat lower in PPOM (1.9 ± 0.6) than in IPOM (2.7 ± 1.0) and were rather variable between IPOM from P6 (3.4 ± 0.9) and P7 (2.0 ± 0.5). The higher concentrations of phytosterols in IPOM from P6 were in accordance with the higher algal biomass and the detection of sympagic HBIs at this station, likely resulting in a proportionally higher contribution of HBI-producing algal taxa (see above). Due to the sampling technique (no prefiltering of samples), POM samples are likely to contain heterotrophic material to some extent (*i.e.*, components of under-ice fauna in PPOM and/or IPOM; in-ice meiofauna, microbial components in IPOM), which can explain the presence of zoosterols in the POM samples. Moreover, some zoosterols can be synthesized in both algae and animal cells (Belt et al., 2018).

3.2. *Apherusa glacialis*

All three FA ratios indicated the dominance of diatom-derived FAs over dinoflagellate-derived FAs (Table 4), irrespective of the sampling location, which is in agreement with previous studies identifying diatoms as an important food item for this species (Scott et al., 1999; Kohlbach et al., 2016). As found for the POM samples, there was large variability in individual FA proportions in *A. glacialis* between the two stations (Fig. 3), pointing to their ability to utilize carbon and food of different origin, and possibly mirroring their varying (trophic) sea-ice association. Contrary to both POM types, the average relative contribution of the diatom-associated FA 16:1(n-7) was twice as high in *A. glacialis* from station P7 compared to P6 (Fig. 4**C**), which was similar to proportions detected in *A. glacialis* from the CAO during late summer, where 16:1(n-7) accounted, on average, for ca. half of the FA content

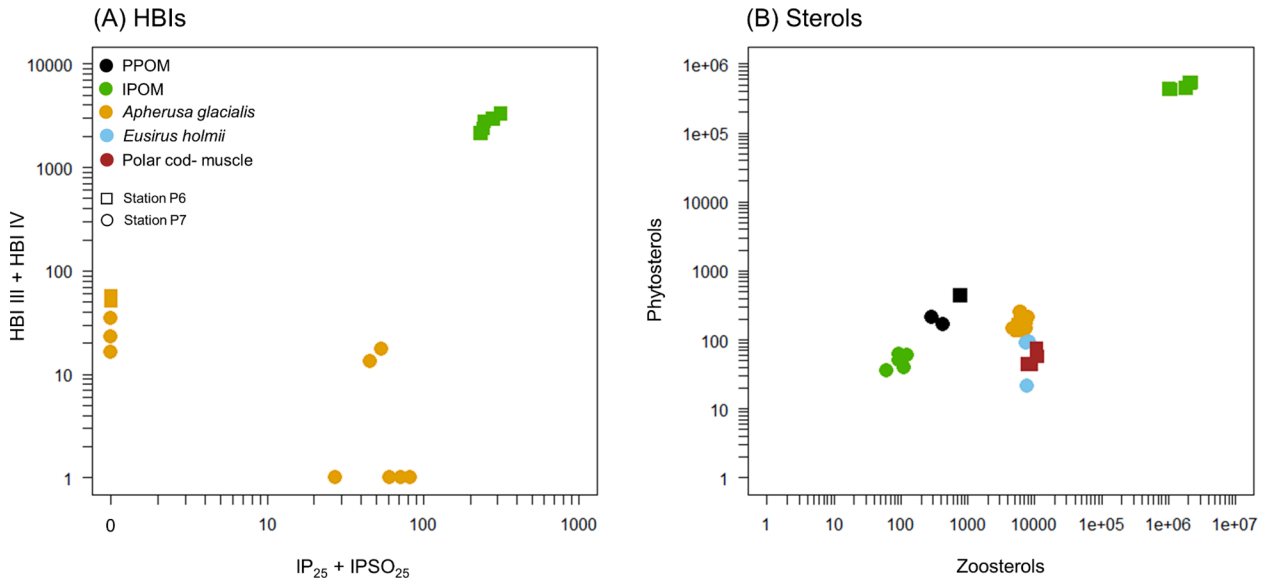

Fig. 6. (A) Concentrations of the sympagic HBIs IP_{25} and $IPSO_{25}$ and the pelagic/MIZ HBIs III and IV in ice-associated particulate organic matter (IPOM; pg mL^{-1}) and the ice amphipod *Apherusa glacialis* (ng g^{-1} dry animal weight). Considered are only samples that either contained sympagic HBIs, pelagic/MIZ HBIs or both (traces of HBI III in one pelagic POM [PPOM] sample, not shown here). (B) Concentrations of phytosterols (sum of brassicasterol, sitosterol, chalinosterol, campesterol) and zoosterols (sum of cholesterol, desmosterol, dehydrocholesterol) in PPOM and IPOM (pg mL^{-1}) and the under-ice fauna (µg g^{-1} dry animal weight). Datapoints represent individual samples.

Table A1
Concentrations (mean ± 1 SD g 100 g $lipid^{-1}$) of the most abundant fatty acids in pelagic particulate organic matter (PPOM), ice-associated POM (IPOM) and under-ice fauna.

Fatty acids	PPOM	IPOM	*Apherusa glacialis*	*Eusirus holmii*	Polar cod-muscle	Polar cod-liver
n	4 (P6: 2, P7: 2)	10 (P6: 5, P7: 5)	20 (P6: 4, P7: 16)	4 (all P7)	4 (all P6)	3 (all P6)
14:0	0.8 ± 0.4	2.5 ± 1.2	1.7 ± 0.6	1.2 ± 0.8	1.3 ± 0.5	4.6 ± 1.2
16:0	1.6 ± 0.3	5.1 ± 2.3	7.9 ± 1.7	6.2 ± 1.1	9.3 ± 0.7	7.3 ± 0.8
16:1 (n-7)	1.1 ± 0.3	5.1 ± 3.8	23.4 ± 10.1	8.1 ± 5.6	1.6 ± 0.4	9.2 ± 1.0
16:4 (n-1)	0.2 ± 0.1	0.8 ± 0.3	0.5 ± 0.3	0.2 ± 0.2	0.004 ± 0.007	0.2 ± 0.01
18:0	0.6 ± 0.2	0.5 ± 0.1	0.5 ± 0.1	0.4 ± 0.1	1.4 ± 0.3	1.0 ± 0.03
18:1 (n-9)	0.7 ± 0.4	0.7 ± 0.3	8.3 ± 2.4	7.8 ± 0.8	3.1 ± 0.3	4.7 ± 0.8
18:4 (n-3)	0.3 ± 0.2	0.7 ± 0.3	0.5 ± 0.2	0.3 ± 0.2	0.5 ± 0.1	1.4 ± 0.4
Σ20:1	0.7 ± 0.8	0.5 ± 0.2	0.7 ± 0.2	4.5 ± 2.6	3.9 ± 1.1	21.9 ± 2.1
20:5 (n-3)	0.5 ± 0.2	3.8 ± 1.5	7.0 ± 1.3	6.9 ± 2.3	9.5 ± 0.2	6.5 ± 0.4
Σ22:1	0.9 ± 1.0	0.4 ± 0.2	0.4 ± 0.2	2.5 ± 1.7	2.2 ± 1.0	17.6 ± 1.8
22:6 (n-3)	0.3 ± 0.1	1.2 ± 0.9	2.6 ± 0.6	7.1 ± 3.9	18.4 ± 2.8	5.9 ± 0.9

(Kohlbach et al., 2016). The opposite trend was found for the contribution of the diatom-associated FA 20:5(n-3), which was twice as high at station P6 compared to P7 (Fig. 4**C**). The third typical diatom-associated FA 16:4(n-1) was also more prominent in the P6 than in the P7 samples. Overall, the diatom signal was stronger in *A. glacialis* from P7 (sum of diatom-associated FAs: 53.6 %) compared to P6 (sum of diatom-associated FAs: 46.3 %). Both dinoflagellate-associated FAs 18:4(n-3) and 22:6(n-3) were significantly higher concentrated in *A. glacialis* at P6 than P7 (Fig. 4**C**). This station-specific difference could not be observed in either of the POM community samples, which could mean that the *A. glacialis* FA profile was not representative of the algal community at the time of sampling. The exact turnover rate of FAs in the amphipod is to date unclear but could be several weeks (Boissonnot et al., 2016, 2019). The observed differences between baseline (*i.e.*, PPOM and IPOM) and consumer can also reflect the (vertical and horizontal) mobility of *A. glacialis*, encountering varying carbon sources, *i.e.*, algal communities, throughout the water column as well as at the underside of the ice. In *A. glacialis* from the CAO, there was a spatial variability in FA proportions, possibly linked to differences in seasonal progression of the ecosystem and different environmental conditions between the Nansen and Amundsen Basins (Kohlbach et al., 2016). In the CAO study, *A. glacialis* from the more northern Amundsen Basin had higher proportions of 16:1(n-7) and lower proportions of all other trophic marker FAs compared to individuals from the Nansen Basin, similar to station P7 versus P6, which was likely the result of lower nutrient and consequently chl *a* concentrations at P7.

In accordance with its previously reported strong association to the sea-ice primary production in both seasonal and perennial sea-ice systems (Søreide et al., 2006; Budge et al., 2008; Kohlbach et al., 2016), *A. glacialis* was the only under-ice fauna species investigated in this study containing detectable amounts of sympagic HBIs (Fig. 6**A**). The lack of sympagic HBIs IP_{25} in all and $IPSO_{25}$ in about half of the samples (eight out of 14 samples) is likely a detection limit issue rather than the absence of these lipids in *A. glacialis*, and further mirrors the distribution of sympagic HBIs in IPOM (see above). Concentrations of the pelagic HBIs were close to the detection limit (0 to 57 ng g^{-1}), and since the sympagic HBIs occurred in distinctly lower concentrations in IPOM (Fig. 6**A**), the failure to detect sympagic HBIs in the consumers was not surprising, unless there was preferential uptake. The presence of $IPSO_{25}$ in *A. glacialis* at P7 (0 to 75 ng g^{-1}) but not the pelagic HBIs III and IV in most of the samples likely reflects a change in diatom species

composition between P6 and P7 (see 3.1). The detection of sympagic HBIs in *A. glacialis* at station P7 but not P6 (Fig. 6**A**), points to a stronger reliance on pelagic carbon sources at P6, supported by the FA profiles, which was likely related to grazing on the under-ice bloom. In contrast, low pelagic productivity left few alternatives to ice algal carbon at P7. This dietary opportunism contradicts the common notion that *A. glacialis* represents a typical ice amphipod with an exclusively sympagic diet (Werner 1997).

The higher phytosterol content in combination with lower zoosterol concentrations compared to the other under-ice fauna species (Fig. 6**B**) further mirrors *A. glacialis'* predominantly herbivorous (detritivorous) lifestyle (Poltermann, 2001; Arndt et al., 2005), assuming that sterol distributions can be used to distinguish algae- versus animal-produced carbon to some extent (Drazen et al., 2008; Ruess and Müller-Navarra, 2019). In contrast to the highly variable FA profiles and HBI content, ratios of zoosterols/phytosterols in *A. glacialis* showed relatively low variability between P6 (40.3 ± 4.7) and P7 (34.5 ± 8.2), suggesting similarities in feeding behaviour, *i.e.*, the reliance on algal- versus animal-derived material, irrespective of the sampling station, prevailing environmental conditions and carbon source/prey availability.

3.3. *Eusirus holmii*

Individuals of *E. holmii* covered a large size range (<10 to 40 mm) and thus likely multiple ontogenetic stages (juveniles and adults, respectively). The largest individual analysed for FAs (40 mm) had a substantially lower diatom signal compared to the other three individuals (particularly low content of 16:1(n-7): 2 %, others: 13 to 23 %), while containing more PUFAs 20:5(n-3) (20 %, others: 10–16 %) and 22:6(n-3) (30 %, others: 8–12 %), indicating a different diet and/or body condition than the smaller individuals. The two samples with individuals below 10 mm in size also had lower PUFA proportions than the second large individual (30 mm), indicating that the proportion of membrane lipids increased with size/age while lipid storage capacities decreased. In support of this assumption, the two adults had a lower percentage of extracted lipids per wet weight (0.6 and 1.3 %) compared to the juveniles (3.1 and 6.0 %). As expected, FA carnivory ratios of 18:1(n-9)/18:1(n-7) (Falk-Petersen et al., 1990; Graeve et al., 1997) increased with size from 3.6 to 10.3, indicating the higher importance of heterotrophic food sources for adult *E. holmii* compared to the younger individuals. In accordance with that result, the ratio of zoo- to phytosterols was also substantially higher in a large individual (351.3) compared to two small animals (85.8 ± 3.1), further suggesting a more pronounced carnivorous lifestyle of older individuals. There was evidence of *Calanus* feeding, concurrent with *E. holmii's* reported predatory lifestyle (Macnaughton et al., 2007), but overall copepod-associated FA proportions were relatively low (Table 4). Interestingly, proportions of the copepod-associated FAs 20:1 and 22:1 were higher in smaller (younger) (up to 17 and 10 %, respectively) than larger (older) *E. holmii* (up to 6 and 3 %, respectively). Based on this, adult *E. holmii* likely targeted other (perhaps larger) prey than *Calanus* copepods, such as amphipods (Macnaughton et al., 2007). Spatial variability in FAs could not be assessed in this study since all individuals were collected at station P6.

The FA profile of the specimen in our study varied greatly from *E. holmii* collected during August in the CAO (Kohlbach et al., 2016). For example, the average relative proportion of 16:1(n-7) in individuals from the CAO was 36 % (here: 15 %). Moreover, in *E. holmii* from the CAO, 82 % of the lipids were storage lipids. In this study, we did not determine the levels of storage versus membrane lipids, but from the high proportions of membrane-bound PUFAs (Table 4), it can be assumed that polar membrane lipids had a greater contribution to the overall lipid content of the animals. These differences likely reflect seasonal differences in diet and body condition as well as geographically-driven dietary variation and/or availability of prey. The animals collected for this study made use of their lipid storage during the long polar winter, while the animals collected in the CAO were likely continuously feeding throughout the summer.

In our study, we did not detect sympagic or pelagic HBIs in *E. holmii*. Brown et al. (2017) suggested that *E. holmii* likely relied mainly on other food sources than sea-ice algae north of Svalbard, which could have also been the case here and has therefore a relatively low relevance for the transfer of ice-derived carbon through the food web. Contrastingly, results derived from stable isotopes indicated a strong reliance on ice-algal carbon for *E. holmii* from the CAO (Kohlbach et al., 2016). Animals inhabiting the CAO have possibly a stronger sea-ice association due to the presence of sea ice year-round and the generally low pelagic productivity that needs to be counterbalanced; during August/September, the time of sampling, ice algal primary production can represent 50 % of the total primary production (Fernández-Méndez et al., 2015). As mentioned above, the seemingly absence of these ice proxies can further point to limitations of the analytical system, *i.e.*, concentrations below the detection limit.

3.4. *Polar cod Boreogadus saida*

As reported previously (Kohlbach et al., 2017), the FA profiles of polar cod tissue (muscle and liver) differed greatly from each other (Fig. 3, Table 4). The liver is known as the main lipid storage organ in polar cod (Hop et al., 1995), accordingly the proportions of storage-associated FAs such as 16:1(n-7) and the copepod-associated FAs were significantly higher in liver versus muscle tissue. In the liver tissue, nearly half of the FAs were copepod-associated FAs, reflecting their strong reliance on *Calanus* spp. as food (Bouchard and Fortier, 2020). This is in line with the diet composition of polar cod from the western Barents Sea during spring (Lønne and Gulliksen, 1989), where *C. glacialis* was found to be the main prey. In our study, there is evidence of a preference for *C. hyperboreus* over other *Calanus* species due to the similarly high proportions of 20:1 and 22:1, a pattern typically found in the largest of the *Calanus* species inhabiting the Barents Sea. Supporting this assumption, *C. hyperboreus* is known to be associated with deep waters (Hirche, 1997; bottom depth > 3000 m at P7) and contributed largely to the *Calanus* copepod biomass at stations P6 and P7.

The diet composition of polar cod can be quite diverse, with differences on a spatial and temporal scale as well as related to ontogeny, reflecting availability and accessibility of their preferred prey as well as their opportunistic feeding behavior (Ajiad and Gjøsæter, 1990; Hop and Gjøsæter, 2013; Matley et al., 2013; Gray et al., 2016; Nakano et al., 2016). In comparison to polar cod collected during summer in the CAO, relative proportions of the diatom-associated FA 16:1(n-7) were at least three times lower in this study in both tissues (CAO muscle: 16 %, liver: 28 %; this study muscle: 3 %, liver: 10 %). The stomach content of the CAO fish was dominated by *A. glacialis* (Kohlbach et al., 2017), which can explain the strong 16:1(n-7) signal, a FA that contributed to almost half of the FA content in the amphipod (Kohlbach et al., 2016). These differences could be explained by varying availability of their prey; *A. glacialis* occurred in high numbers in the CAO (David et al., 2015), and might have simply been less abundant or less easily accessible underneath the thinner, ridged ice in the Barents Sea. Furthermore, the fish in the present study was in a later ontogenetic stage, based on their larger size (CAO: average 78 mm, this study: average 118 mm) and wet weight (CAO: average 3 g, this study: average 11 g). Larger polar cod have a greater prey diversity, including amphipods such as *Themisto libellula* (Renaud et al., 2012; Dalpadado et al., 2016).

No HBIs could be detected in the polar cod muscle tissue, which might point to concentrations below the detection limit as mentioned above. The lack of sympagic HBIs could further be related to the seemingly lower reliance on *A. glacialis*, which likely transferred the sea-ice signal in the individuals from the CAO, where the ice algal contribution was quantified with up to 65 % in the muscle tissue based on FA-specific stable isotope analysis (Kohlbach et al., 2017). There might also be a moderate to low importance of sympagic food for polar cod in the

sampling region, as polar cod sampled during August and November/December in the Barents Sea did also not contain any detectable amounts of HBIs, with the exception of pelagic HBIs in low concentrations in few individuals (unpubl. data). Despite their presence underneath the sea ice, the polar cod in our study might have had a stronger reliance on pelagic food sources, as also suggested for juvenile polar cod from the Barents and Beaufort Seas (Hop and Gjøsæter, 2013; Graham et al., 2014), presumably feeding on copepods utilizing the under-ice bloom at P6. As discussed above, these results might reflect the spatial variability in food composition with a larger probability and requirement to incorporate sympagic food items in a sea ice-dominated ecosystem such as the CAO. Sterol composition and high zoosterol/phytosterol ratios (181.7 ± 25.5) showed relatively little variability between the four polar cod individuals (Fig. 6**B**). The general similarity in trophic marker composition among muscle and liver tissue, respectively, points to a resemblance in food sources utilized by the different individuals collected at station P6.

4. Conclusions

In this study, trophic marker evidence of the reliance on sympagic carbon was found in the under-ice amphipod *Apherusa glacialis*, confirming its previously reported trophic sea-ice association. The low concentrations of sympagic HBIs in *A. glacialis* along with their absence in the amphipod *Eusirus holmii* and polar cod possibly reflect a low contribution of HBI-producing taxa to the sea-ice diatom community. High spatial variability in FA profiles and in the presence of sympagic HBIs suggest that the dietary composition of *A. glacialis* might be rather flexible and opportunistic, and perhaps less ice-algal dependent compared to regions that are ice-covered year-round. In comparison to a perennially ice-covered system, a lower importance of sympagic carbon to the diet of the investigated under-ice fauna species and, in general, for trophic processes in the seasonally ice-covered Barents Sea might be expected since pelagic carbon sources are abundant during the productive season. In accordance with this assumption, an under-ice bloom occurring at station P6 likely offered sufficient carbon and food sources that might have been preferably utilized by the under-ice fauna, suggesting that such species are well adapted to exploiting pelagic food items. In contrast, the less productive pelagic system at P7 likely resulted in a stronger reliance on sympagic carbon, as shown for *A. glacialis*. These results imply that ice-associated species do not necessarily rely exclusively on sympagic carbon: When following the Transpolar drift, *A. glacialis* is likely to traverse different productivity regimes and adopt the ability to switch between sympagic and pelagic food items. This trophic plasticity might provide them with an advantage regarding continued sea-ice retreat and accompanied changes in sea-ice primary production but could potentially also impact their nutritional value for higher trophic levels depending on the food quality of their carbon sources.

Compared to level sea ice, sea-ice ridges as encountered in our study particularly facilitate the attachment of algae by providing greater surface area sheltered from harsh environmental surroundings (Fernández-Méndez et al., 2018), resulting in sympagic algae communities with high biomass and diversity, which in turn attract herbivorous ice fauna and consequently their predators (Hop et al., 2000; Gradinger et al., 2010). Sea-ice ridges are generally understudied despite their importance as structural features of the Arctic sea-ice habitat (Hutter et al., 2019; Lange et al. under review). Hence, it is unclear whether environmental changes of the Arctic icescape will eventually benefit or hamper the development of sea-ice ridges (Wadhams and Toberg, 2012; Fernández-Méndez et al., 2018; Lange et al. under review). Regardless of changes in sea-ice ridges in future decades, environmental change will have an impact on ice-associated fauna, their trophic interactions and the energy flow through the entire Arctic food web. Our study contributes to our current knowledge on the usage of sea-ice ridges as a feeding ground for ice-associated fauna and encourages further investigations of the sympagic habitat to gain information about potential differences in the importance of ice-associated algae for food-web functioning during different seasons, regions and in comparison to level sea ice.

Declaration of Competing Interest

The authors declare that they have no known competing financial interests or personal relationships that could have appeared to influence the work reported in this paper.

Data availability

Data will be made available on request.

Acknowledgements

The authors thank the captain and the crew of RV *Kronprins Haakon* for their excellent support at sea during the Nansen Legacy seasonal cruise Q2. We also thank Julia Giebichenstein, Helene Thorstensen and Robynne Nowicki for their help with sampling.

Thanks to Miriam Marquart, Yasemin Bodur and Natalie Summers for sampling and processing of chl *a* samples. We thank the members of the scientific dive team (Amalia Keck Al-Habahbeh, Peter Leopold and Mikko Vihtakari) for collection of samples below sea ice and are grateful for pictures of the under-ice environment and divers taken by Peter Leopold. Furthermore, we thank the Chemistry Lab Section at Akvaplan-niva under the leadership of Lisa Torske for the analysis of FA for this study. We thank the editor Enrique Curchitser and the three reviewers for providing helpful comments and suggestions during the review process.

Funding information

This work was funded by the Research Council of Norway through the project The Nansen Legacy (RCN # 276730). Contributions by STB were funded by the UK's Natural Environment Research Council MOSAiC-Thematic project SYM-PEL: "Quantifying the contribution of sympagic versus pelagic diatoms to Arctic food webs and biogeochemical fluxes: application of source-specific highly branched isoprenoid biomarkers" (NE/S002502/1).

Author contribution

This study was designed by DK, PA and HH. Sampling was conducted by HH, DK and PA; HH and PA provided sampling logistics. LS did the HBI and sterol analyses and data evaluation with the help of STB. STB provided laboratory materials, methodological expertise, and laboratory space. Data analyses and figure assemblage was done by DK with the help of the other authors. DK is the main author of this paper. All authors contributed significantly to data interpretation and to the writing of the manuscript.

Appendix

See Table A1.

References

Aarflot, J.M., Skjoldal, H.R., Dalpadado, P., Skern-Mauritzen, M., Fields, D., 2018. Contribution of *Calanus* species to the mesozooplankton biomass in the Barents Sea. ICES J. Mar. Sci. 75 (7), 2342–2354.

Ainley, D.G., Tynan, C.T., Stirling, I., 2003. Sea ice: a critical habitat for polar marine mammals and birds. In: Thomas, D.N., Dieckmann, G.S. (Eds.), Sea Ice: an Introduction to Its Physics, Chemistry, Biology, and Geology. Blackwell, pp. 240–266.

Ajiad, A.M., and Gjøsæter, H. 1990. Diet of polar cod, *Boreogadus saida*, in the Barents Sea related to fish size and geographical distribution. International Council for the Exploration of the Sea, Council Meeting 1990/G:48, 9 pp.

Arndt, C.E., Berge, J., Brandt, A., 2005. Mouthpart-atlas of Arctic sympagic amphipods—trophic niche separation based on mouthpart morphology and feeding ecology. J. Crustac. Biol. 25 (3), 401–412.
Arndt, C.E., Swadling, K.M., 2006. Crustacea in Arctic and Antarctic sea ice: distribution, diet and life history strategies. Adv. Mar. Biol. 51, 197–315.
Arrigo, K.R., 2017. Sea ice as a habitat for primary producers. In: Thomas, D.N. (Ed.), Sea ice. Wiley-Blackwell, pp. 352–369.
Årthun, M., Eldevik, T., Smedsrud, L., Skagseth, Ø., Ingvaldsen, R.B., 2012. Quantifying the influence of Atlantic heat on Barents Sea ice variability and retreat. J. Clim. 25, 4736–4743.
Asbjørnsen, H., Årthun, M., Skagseth, Ø., Eldevik, T., 2020. Mechanisms underlying recent Arctic Atlantification. Geophys. Res. Lett. 47 (15) e2020GL088036.
Barber, D.G., Hop, H., Mundy, C.J., Else, B., Dmitrenko, I.A., Tremblay, J.-E., Ehn, J.K., Assmy, P., Daase, M., Candlish, L.M., Rysgaard, S., 2015. Selected physical, biological and biogeochemical implications of a rapidly changing Arctic Marginal Ice Zone. Prog. Oceanogr. 139, 122–150.
Barton, B.I., Lenn, Y.-D., Lique, C.J., 2018. Observed Atlantification of the Barents Sea causes the polar front to limit the expansion of winter sea ice. J. Phys. Oceanogr. 48, 1849–1866.
Belt, S.T., 2018. Source-specific biomarkers as proxies for Arctic and Antarctic sea ice. Org. Geochem. 125, 277–298.
Belt, S.T., Brown, T.A., Rodriguez, A.N., Sanz, P.C., Tonkin, A., Ingle, R., 2012. A reproducible method for the extraction, identification and quantification of the Arctic sea ice proxy IP_{25} from marine sediments. Anal. Meth. 4 (3), 705–713.
Belt, S.T., Brown, T.A., Smik, L., Assmy, P., Mundy, C.J., 2018. Sterol identification in floating Arctic sea ice algal aggregates and the Antarctic sea ice diatom *Berkeleya adeliensis*. Org. Geochem. 118, 1–3.
Berge, J., Varpe, Ø., Moline, M.A., Wold, A., Renaud, P.E., Daase, M., Falk-Petersen, S., 2012. Retention of ice-associated amphipods: possible consequences for an ice-free Arctic Ocean. Biol. Lett. 8 (6), 1012–1015.
Beuchel, F., Lønne, O.J., 2002. Population dynamics of the sympagic amphipods *Gammarus wilkitzkii* and *Apherusa glacialis* in sea ice north of Svalbard. Polar Biol. 25 (4), 241–250.
Bluhm, B.A., Swadling, K.M., Gradinger, R.R., 2017. Sea ice as a habitat for macrograzers. In: Thomas, D.N. (Ed.), Sea ice. Wiley-Blackwell, pp. 394–414.
Boissonnot, L., Niehoff, B., Hagen, W., Søreide, J.E., Graeve, M., 2016. Lipid turnover reflects life-cycle strategies of small-sized Arctic copepods. J. Plankton Res. 38 (6), 1420–1432.
Boissonnot, L., Niehoff, B., Ehrenfels, B., Søreide, J.E., Hagen, W., Graeve, M., 2019. Lipid and fatty acid turnover of the pteropods *Limacina helicina, L. retroversa* and *Clione limacina* from Svalbard waters. Mar. Ecol. Prog. Ser. 609, 133–149.
Bouchard, C., Fortier, L., 2020. The importance of *Calanus glacialis* for the feeding success of young polar cod: a circumpolar synthesis. Polar Biol. 43 (8), 1095–1107.
Bradstreet, M.S., Cross, W.E., 1982. Trophic relationships at high Arctic ice edges. Arctic 35, 1–12.
Brett, M., Müller-Navarra, D., 1997. The role of highly unsaturated fatty acids in aquatic foodweb processes. Freshwater Biol. 38 (3), 483–499.
Brown, T.A., Assmy, P., Hop, H., Wold, A., Belt, S.T., 2017. Transfer of ice algae carbon to ice-associated amphipods in the high-Arctic pack ice environment. J. Plankton Res. 39 (4), 664–674.
Brown, T.A., Belt, S.T., 2012. Identification of the sea ice diatom biomarker IP_{25} in Arctic benthic macrofauna: direct evidence for a sea ice diatom diet in Arctic heterotrophs. Polar Biol. 35 (1), 131–137.
Brown, T.A., Belt, S.T., Tatarek, A., Mundy, C., 2014. Source identification of the Arctic sea ice proxy IP_{25}. Nature Commun. 5, 1–7.
Brown, T.A., Galicia, M.P., Thiemann, G.W., Belt, S.T., Yurkowski, D.J., Dyck, M.G., Derocher, A., 2018. High contributions of sea ice derived carbon in polar bear (*Ursus maritimus*) tissue. PloS One 13 (1), e0191631.
Budge, S.M., Wooller, M.J., Springer, A.M., Iverson, S.J., McRoy, C.P., Divoky, G.J., 2008. Tracing carbon flow in an arctic marine food web using fatty acid-stable isotope analysis. Oecologia 157 (1), 117–129.
Dahlke, F.T., Butzin, M., Nahrgang, J., Puvanendran, V., Mortensen, A., Pörtner, H.-O., Storch, D., 2018. Northern cod species face spawning habitat losses if global warming exceeds 1.5 °C. Sci. Adv. 4 (11), eaas8821.
Dalpadado, P., Ingvaldsen, R.B., Stige, L.C., Bogstad, B., Knutsen, T., Ottersen, G., Ellertsen, B., 2012. Climate effects on Barents Sea ecosystem dynamics. ICES J. Mar. Sci. 69 (7), 1303–1316.
Dalpadado, P., Hop, H., Rønning, J., Pavlov, V., Sperfeld, E., Buchholz, F., Rey, A., Wold, A., 2016. Distribution and abundance of euphausiids and pelagic amphipods in Kongsfjorden, Isfjorden and Rijpfjorden (Svalbard) and changes in their relative importance as key prey in a warming marine ecosystem. Polar Biol. 39 (10), 1765–1784.
Dalpadado, P., Arrigo, K.R., van Dijken, G.L., Skjoldal, H.R., Bagøien, E., Dolgov, A.V., Prokopchuk, I.P., Sperfeld, E., 2020. Climate effects on temporal and spatial dynamics of phytoplankton and zooplankton in the Barents Sea. Prog. Oceanogr. 185, 102320.
Dalsgaard, J., St John, M., Kattner, G., Muller-Navarra, D., Hagen, W., 2003. Fatty acid trophic markers in the pelagic marine environment. Adv. Mar. Biol. 46, 227–237.
David, C., Lange, B.A., Rabe, B., Flores, H., 2015. Community structure of under-ice fauna in the Eurasian central Arctic Ocean in relation to environmental properties of sea-ice habitats. Mar. Ecol. Prog. Ser. 522, 15–32.
David, C., Lange, B.A., Krumpen, T., Schaafsma, F., van Franeker, J.A., Flores, H., 2016. Under-ice distribution of polar cod *Boreogadus saida* in the central Arctic Ocean and their association with sea-ice habitat properties. Polar Biol. 39 (6), 981–994.
Drazen, J.C., Phleger, C.F., Guest, M.A., Nichols, P.D., 2008. Lipid, sterols and fatty acid composition of abyssal holothurians and ophiuroids from the North-East Pacific Ocean: food web implications. Comp. Biochem. Physiol. B 151 (1), 79–87.
Drivdal, M., Kunisch, E.H., Bluhm, B.A., Gradinger, R.R., Falk-Petersen, S., Berge, J., 2021. Connections to the deep: Deep vertical migrations, an important part of the life cycle of *Apherusa glacialis*, an Arctic ice-associated amphipod. Front. Mar. Sci. 8, 772766.
Dupont, F., 2012. Impact of sea-ice biology on overall primary production in a biophysical model of the pan-Arctic Ocean. J. Geophys. Res. Oceans 117 (C8), C00D17.
Dupont, N., Durant, J.M., Langangen, Ø., Gjøsæter, H., Stige, L.C., Anderson, E., 2020. Sea ice, temperature, and prey effects on annual variations in mean lengths of a key Arctic fish, *Boreogadus saida*, in the Barents Sea. J. Mar. Sci. 77 (5), 1796–1805.
Ehrlich, J., Schaafsma, F.L., Bluhm, B.A., Peeken, I., Castellani, G., Brandt, A., et al., 2020. Sympagic fauna in and under Arctic pack ice in the annual sea-ice system of the new Arctic. Front. Mar. Sci. 7, 452.
Ehrlich, J., Bluhm, B.A., Peeken, I., Massicotte, P., Schaafsma, F.L., Castellani, G., Brandt, A., Flores, H., 2021. Sea-ice associated carbon flux in Arctic spring. Elem. Sci. Anthr. 9 (1), 00169.
Eriksen, E., Ingvaldsen, R.B., Nedreaas, K., Prozorkevich, D., 2015. The effect of recent warming on polar cod and beaked redfish juveniles in the Barents Sea. Reg. Stud. Mar. Sci. 2, 105–112.
Eriksen, E., Skjoldal, H.R., Gjøsæter, H., Primicerio, R., 2017. Spatial and temporal changes in the Barents Sea pelagic compartment during the recent warming. Prog. Oceanogr. 151, 206–226.
Ershova, E.A., Kosobokova, K.N., Banas, N.S., Ellingsen, I., Niehoff, B., Hildebrandt, N., Hirche, H.-J., 2021. Sea ice decline drives biogeographical shifts of key *Calanus* species in the central Arctic Ocean. Glob. Change Biol. 27 (10), 2128–2143.
Falk-Petersen, S., Hopkins, C., Sargent, J.R., 1990. Trophic relationships in the pelagic, Arctic food web. In: Barnes, M., Gibson, R.N. (Eds.), Trophic Relationships in the Marine Environment. Aberdeen University Press, Aberdeen, pp. 315–333.
Falk-Petersen, S., Sargent, J.R., Henderson, J., Hegseth, E.N., Hop, H., Okolodkov, Y.B., 1998. Lipids and fatty acids in ice algae and phytoplankton from the Marginal Ice Zone in the Barents Sea. Polar Biol. 20 (1), 41–47.
Fernández-Méndez, M., Katlein, C., Rabe, B., Nicolaus, M., Peeken, I., Bakker, K., Flores, H., Boetius, A., 2015. Photosynthetic production in the central Arctic Ocean during the record sea-ice minimum in 2012. Biogeosciences 12 (11), 3525–3549.
Fernández-Méndez, M., Olsen, L.M., Kauko, H.M., Meyer, A., Rösel, A., Merkouriadi, I., Mundy, C.J., Ehn, J.K., Johansson, A.M., Wagner, P.M., Ervik, Å., Sorrell, B.K., Duarte, P., Wold, A., Hop, H., Assmy, P., 2018. Algal hot spots in a changing Arctic Ocean: Sea-ice ridges and the snow-ice interface. Front. Mar. Sci. 5.
Folch, J., Lees, M., Stanley, G.H.S., 1957. A simple method for the isolation and purification of total lipides from animal tissues. J. Biol. Chem. 226 (1), 497–509.
Gjøsæter, H., Huserbråten, M., Vikebø, F., Eriksen, E., 2020. Key processes regulating the early life history of Barents Sea polar cod. Polar Biol. 43 (8), 1015–1027.
Gradinger, R.R., Bluhm, B.A., 2004. In-situ observations on the distribution and behavior of amphipods and Arctic cod (*Boreogadus saida*) under the sea ice of the High Arctic Canada Basin. Polar Biol. 27, 595–603.
Gradinger, R.R., Meiners, K., Plumley, G., Zhang, Q., Bluhm, B.A., 2005. Abundance and composition of the sea-ice meiofauna in off-shore pack ice of the Beaufort Gyre in summer 2002 and 2003. Polar Biol. 28 (3), 171–181.
Gradinger, R.R., Bluhm, B.A., Iken, K., 2010. Arctic sea-ice ridges—Safe heavens for sea-ice fauna during periods of extreme ice melt? Deep Sea Res. II 57 (1–2), 86–95.
Graeve, M., Kattner, G., Piepenburg, D., 1997. Lipids in Arctic benthos: does the fatty acid and alcohol composition reflect feeding and trophic interactions? Polar Biol. 18 (1), 53–61.
Graham, C., Oxtoby, L., Wang, S.W., Budge, S.M., Wooller, M.J., 2014. Sourcing fatty acids to juvenile polar cod (*Boreogadus saida*) in the Beaufort Sea using compound-specific stable carbon isotope analyses. Polar Biol. 37 (5), 697–705.
Gray, B.P., Norcross, B.L., Blanchard, A.L., Beaudreau, A.H., Seitz, A.C., 2016. Variability in the summer diets of juvenile polar cod (*Boreogadus saida*) in the northeastern Chukchi and western Beaufort Seas. Polar Biol. 39 (6), 1069–1080.
Greenacre, M., 2017. Correspondence analysis in practice. CRC Press.
Greenacre, M., Primicerio, R., 2014. Multivariate analysis of ecological data. Fundacion BBVA, Bilbao.
Gulati, RAMESH, Demott, WILLIAM, 1997. The role of food quality for zooplankton: remarks on the state-of-the-art, perspectives and priorities. Freshwater Biol. 38 (3), 753–768.
Henderson, R.J., Hegseth, E.N., Park, M.T., 1998. Seasonal variation in lipid and fatty acid composition of ice algae from the Barents Sea. Polar Biol. 20 (1), 48–55.
Hirche, H.-J., 1997. Life cycle of the copepod *Calanus hyperboreus* in the Greenland Sea. Mar. Biol. 128 (4), 607–618.
Holm-Hansen, O., Riemann, B., 1978. Chlorophyll *a* determination: Improvements in methodology. Oikos 30, 438–447.
Hop, H., Wold, A., Vihtakari, M., Daase, M., Kwasniewski, S., Gluchowska, M., et al., 2019. Zooplankton in Kongsfjorden (1996–2016) in relation to climate change. In: Hop, H., Wiencke, C. (Eds.), The Ecosystem of Kongsfjorden, Svalbard. Springer, pp. 229–300.
Hop, H., Gjøsæter, H., 2013. Polar cod (*Boreogadus saida*) and capelin (*Mallotus villosus*) as key species in marine food webs of the Arctic and the Barents Sea. Mar. Biol. Res. 9 (9), 878–894.
Hop, H., Trudeau, V.L., Graham, M., 1995. Spawning energetics of Arctic cod (*Boreogadus saida*) in relation to seasonal development of the ovary and plasma sex steroid levels. Can. J. Fish. Aquat. Sci. 52 (3), 541–550.

Hop, H., Poltermann, M., Lønne, O.J., Falk-Petersen, S., Korsnes, R., Budgell, W.P., 2000. Ice amphipod distribution relative to ice density and under-ice topography in the northern Barents Sea. Polar Biol. 23 (5), 357–367.
Hop, H., Vihtakari, M., Bluhm, B.A., Daase, M., Gradinger, R.R., Melnikov, I.A., 2021. Ice-associated amphipods in a pan-Arctic scenario of declining sea ice. Front. Mar. Sci. 8, 743152.
Huserbråten, M., Eriksen, E., Gjøsæter, H., Vikebø, F., 2019. Polar cod in jeopardy under the retreating Arctic sea ice. Commun. Biol. 2, 1–8.
Hutter, N., Zampieri, L., Losch, M., 2019. Leads and ridges in Arctic sea ice from RGPS data and a new tracking algorithm. Cryosphere 13 (2), 627–645.
Ingvaldsen, R.B., Assmann, K.M., Primicerio, R., Fossheim, M., Polyakov, I.V., Dolgov, A. V., et al., 2021. Physical manifestations and ecological implications of Arctic Atlantification. Nat. Rev. Earth Environ. 2, 874–889.
Jakubas, D., Głuchowska, M., Wojczulanis-Jakubas, K., Karnovsky, N.J., Keslinka, L., Kidawa, D., Walkusz, W., Boehnke, R., Cisek, M., Kwasniewski, S., Stempniewicz, L., 2011. Foraging effort does not influence body condition and stress level in little auks. Mar. Ecol. Prog. Ser. 432, 277–290.
Ji, R., Jin, M., Varpe, Ø., 2013. Sea ice phenology and timing of primary production pulses in the Arctic Ocean. Glob. Change Biol. 19 (3), 734–741.
Koenigstein, S. (2020). Arctic marine ecosystems, climate change impacts, and governance responses: An integrated perspective from the Barents Sea. In: E. Pongrácz, E.; Pavlov, V., Hänninen, N. (Eds.), Arctic Marine Sustainability. Springer, pp. 45-71.
Kohlbach, D., Graeve, M., Lange, B.A., David, C., Peeken, I., Flores, H., 2016. The importance of ice algae-produced carbon in the central Arctic Ocean ecosystem: Food web relationships revealed by lipid and stable isotope analyses. Limnol. Oceanogr. 61 (6), 2027–2044.
Kohlbach, D., Schaafsma, F.L., Graeve, M., Lebreton, B., Lange, B.A., David, C., Vortkamp, M., Flores, H., 2017. Strong linkage of polar cod (*Boreogadus saida*) to sea ice algae-produced carbon: evidence from stomach content, fatty acid and stable isotope analyses. Prog. Oceanogr. 152, 62–74.
Kohlbach, D., Ferguson, S.H., Brown, T.A., Michel, C., 2019. Landfast sea ice-benthic coupling during spring and potential impacts of system changes on food web dynamics in Eclipse Sound, Canadian Arctic. Mar. Ecol. Prog. Ser. 627, 33–48.
Kohlbach, D., Hop, H., Wold, A., Schmidt, K., Smik, L., Belt, S.T., Keck Al-Hababheh, A., Woll, M., Graeve, M., Dąbrowska, A.M., Tatarek, A., Atkinson, A., Assmy, P., 2021a. Multiple trophic markers trace dietary carbon sources in Barents Sea zooplankton during late summer. Front. Mar. Sci. 7, 1216.
Kohlbach, D., Schmidt, K., Hop, H., Wold, A., Keck-Habahbeh, A., Belt, S.T., et al., 2021b. Winter carnivory and diapause counteract the reliance of Barents Sea zooplankton on ice algae. Front. Mar. Sci. 8, 266.
Kovacs, K.M., Lydersen, C., Overland, J.E., Moore, S.E., 2011. Impacts of changing sea-ice conditions on Arctic marine mammals. Mar. Biodiv. 41 (1), 181–194.
Kumar, A., Yadav, J., Mohan, R., 2021. Spatio-temporal change and variability of Barents-Kara sea ice, in the Arctic: Ocean and atmospheric implications. Sci. Total Environ. 753, 142046.
Kunisch, E.H., Bluhm, B.A., Daase, M., Gradinger, R.R., Hop, H., Melnikov, I.A., Varpe, Ø., Berge, J., Irigoien, X., 2020. Pelagic occurrences of the ice amphipod *Apherusa glacialis* throughout the Arctic. J. Plankton Res. 42 (1), 73–86.
Laidre, K.L., Stern, H., Kovacs, K.M., Lowry, L., Moore, S.E., Regehr, E.V., Ferguson, S.H., Wiig, Ø., Boveng, P., Angliss, R.P., Born, E.W., Litovka, D., Quakenbush, L., Lydersen, C., Vongraven, D., Ugarte, F., 2015. Arctic marine mammal population status, sea ice habitat loss, and conservation recommendations for the 21st century. Conserv. Biol. 29 (3), 724–737.
Lange, B.A., Salganik, E., Macfarlane, A., Schneebeli, M., Høyland, K, Gardner, J., et al. Snowmelt contributes to Arctic first-year ice ridge mass balance and rapid consolidation during summer melt. Under review in Elementa Sci. Anthr.
Lange, B.A., Katlein, C., Nicolaus, M., Peeken, I., Flores, H., 2016. Sea ice algae chlorophyll *a* concentrations derived from under-ice spectral radiation profiling platforms. J. Geophys. Res. Oceans 121 (12), 8511–8534.
Lange, B.A., Katlein, C., Castellani, G., Fernández-Méndez, M., Nicolaus, M., Peeken, I., et al., 2017. Characterizing spatial variability of ice algal chlorophyll *a* and net primary production between sea ice habitats using horizontal profiling platforms. Front. Mar. Sci. 4, 349.
Lee, R., Hagen, W., Kattner, G., 2006. Lipid storage in marine zooplankton. Mar. Ecol. Prog. Ser. 307, 273–306.
Leu, E., Søreide, J.E., Hessen, D.O., Falk-Petersen, S., Berge, J., 2011. Consequences of changing sea-ice cover for primary and secondary producers in the European Arctic shelf seas: timing, quantity, and quality. Prog. Oceanogr. 90 (1-4), 18–32.
Lønne, O.J., Gabrielsen, G.W., 1992. Summer diet of seabirds feeding in sea-ice-covered waters near Svalbard. Polar Biol. 12, 685–692.
Lønne, O.J., Gulliksen, B., 1989. Size, age and diet of polar cod, *Boreogadus saida* (Lepechin 1773), in ice covered waters. Polar Biol. 9 (3), 187–191.
Lønne, O.J., Gulliksen, B., 1991. On the distribution of sympagic macro-fauna in the seasonally ice covered Barents Sea. Polar Biol. 11, 457–469.
Lörz, A.-N., Tandberg, A.H.S., Willassen, E., Driskell, A., 2018. *Rhachotropis* (Eusiroidea, Amphipoda) from the North East Atlantic. Zookeys 731, 75–101.
Lund-Hansen, L.C., Hawes, I., Nielsen, M.H., Sorrell, B.K., 2017. Is colonization of sea ice by diatoms facilitated by increased surface roughness in growing ice crystals? Polar Biol. 40, 593–602.
Macnaughton, M.O., Thormar, J., Berge, J., 2007. Sympagic amphipods in the Arctic pack ice: redescriptions of *Eusirus holmii* Hansen, 1887 and *Pleusymtes karstensi* (Barnard, 1959). Polar Biol. 30 (8), 1013–1025.
Matley, J.K., Fisk, A.T., Dick, T.A., 2013. The foraging ecology of Arctic cod (*Boreogadus saida*) during open water (July–August) in Allen Bay, Arctic Canada. Mar. Biol. 160 (11), 2993–3004.
McBride, M.M., Filin, A., Titov, O.V., and Stiansen, J.E. 2014. IMR/PINRO update of the Joint Norwegian-Russian environmental status report on the Barents Sea Ecosystem.
McMahon, K.W., Ambrose WG, J.r., Johnson, B.J., Sun, M.Y., Lopez, G.R., Clough, L.M., Carroll, M.L., 2006. Benthic community response to ice algae and phytoplankton in Ny Ålesund. Svalbard. *Mar. Ecol. Prog. Ser.* 310, 1–14.
Melnikov, I.A., Chernova, N.V., 2013. Characteristics of under-ice swarming of polar cod *Boreogadus saida* (Gadidae) in the Central Arctic Ocean. J. Ichthyol. 53 (1), 7–15.
Møller, E.F., Nielsen, T.G., 2020. Borealization of Arctic zooplankton—smaller and less fat zooplankton species in Disko Bay, Western Greenland. Limnol. Oceanogr. 65 (6), 1175–1188.
Moran, S.B., Lomas, M.W., Kelly, R.P., Gradinger, R.R., Iken, K., Mathis, J.T., 2012. Seasonal succession of net primary productivity, particulate organic carbon export, and autotrophic community composition in the eastern Bering Sea. Deep Sea Res. II 65, 84–97.
Reuss, N., Poulsen, L., 2002. Evaluation of fatty acids as biomarkers for a natural plankton community. A field study of a spring bloom and a post-bloom period off West Greenland. Mar. Biol. 141 (3), 423–434.
Nakano, T., Matsuno, K., Nishizawa, B., Iwahara, Y., Mitani, Y., Yamamoto, J., Sakurai, Y., Watanuki, Y., 2016. Diets and body condition of polar cod (*Boreogadus saida*) in the northern Bering Sea and Chukchi Sea. Polar Biol. 39 (6), 1081–1086.
Ogloff, W.R., Ferguson, S.H., Tallman, R.F., Davoren, G.K., 2020. Diet of capelin (*Mallotus villosus*) in the Eastern Canadian Arctic inferred from stomach contents and stable isotopes. Polar Biol. 43 (9), 1273–1285.
Oksanen, J., Blanchet, F.G., Friendly, M., Kindt, R., Legendre, P., McGlinn, D., et al. 2020. vegan: Community Ecology Package. R package, version 2.5-7. https://CRAN.R-project.org/package=vegan.
Onarheim, I.H., Årthun, M., 2017. Toward an ice-free Barents Sea. Geophys. Res. Lett. 44 (16), 8387–8395.
Pagano, A.M., Williams, T.M., 2021. Physiological consequences of Arctic sea ice loss on large marine carnivores: unique responses by polar bears and narwhals. J. Exp. Biol. 224 (Suppl_1), jeb228049.
Poltermann, M., 2001. Arctic sea ice as feeding ground for amphipods–food sources and strategies. Polar Biol. 24 (2), 89–96.
R Core Team, 2021. R: A language and environment for statistical computing. R Foundation for Statistical Computing, Vienna, Austria.
Ratkova, T.N., Wassmann, P., 2005. Sea ice algae in the White and Barents seas: composition and origin. Polar Res. 24 (1-2), 95–110.
Renaud, P.E., Berge, J., Varpe, Ø., Lønne, O.J., Nahrgang, J., Ottesen, C., et al., 2012. Is the poleward expansion by Atlantic cod and haddock threatening native polar cod, *Boreogadus saida*? Polar Biol. 35, 401–412.
Ruess, L., Müller-Navarra, D., 2019. Essential biomolecules in food webs. Front. Ecol. Evol. 7, 269.
Rysgaard, S., Kühl, M., Glud, R.N., Hansen, J.W., 2001. Biomass, production and horizontal patchiness of sea ice algae in a high-Arctic fjord (Young Sound, NE Greenland). Mar. Ecol. Prog. Ser. 223, 15–26.
Sargent, J.R., Falk-Petersen, S., 1988. The lipid biochemistry of calanoid copepods. Hydrobiol. 167 (168), 101–114.
Sargent, J.R., 1995. Origins and functions of (n-3) polyunsaturated fatty acids in marine organisms. American Oil Chemists Society Press, pp. 250–261.
Schmidt, K., Brown, T.A., Belt, S.T., Ireland, L., Taylor, K., Thorpe, S., et al., 2018. Do pelagic grazers benefit from sea ice? Insights from the Antarctic sea ice proxy $IPSO_{25}$. Biogeosciences 15, 1987–2006.
Scott, C.L., Falk-Petersen, S., Sargent, J.R., Hop, H., Lønne, O.J., Poltermann, M., 1999. Lipids and trophic interactions of ice fauna and pelagic zooplankton in the marginal ice zone of the Barents Sea. Polar Biol. 21 (2), 65–70.
Smith, R.E., Cavaletto, J.F., Eadie, B., Gardner, W.S., 1993. Growth and lipid composition of high Arctic ice algae during the spring bloom at Resolute, Northwest Territories, Canada. Mar. Ecol. Prog. Ser. 97, 19–29.
Song, H., Ji, R., Jin, M., Li, Y., Feng, Z., Varpe, Ø., Davis, C.S., 2021. Strong and regionally distinct links between ice-retreat timing and phytoplankton production in the Arctic Ocean. Limnol. Oceanogr. 66 (6), 2498–2508.
Søreide, J.E., Hop, H., Carroll, M.L., Falk-Petersen, S., Hegseth, E.N., 2006. Seasonal food web structures and sympagic–pelagic coupling in the European Arctic revealed by stable isotopes and a two-source food web model. Prog. Oceanogr. 71 (1), 59–87.
Søreide, J.E., Leu, E., Berge, J., Graeve, M., Falk-Petersen, S., 2010. Timing of blooms, algal food quality and *Calanus glacialis* reproduction and growth in a changing Arctic. Glob. Change Biol. 16 (11), 3154–3163.
Søreide, J.E., Carroll, M.L., Hop, H., Ambrose, W.G., Hegseth, E.N., Falk-Petersen, S., 2013. Sympagic-pelagic-benthic coupling in Arctic and Atlantic waters around Svalbard revealed by stable isotopic and fatty acid tracers. Mar. Biol. Res. 9 (9), 831–850.
Stige, L.C., Eriksen, E., Dalpadado, P., Ono, K., Bartolino, V., 2019. Direct and indirect effects of sea ice cover on major zooplankton groups and planktivorous fishes in the Barents Sea. ICES J. Mar. Sci. 76 (Supplement_1), i24–i36.
Stübing, D., Hagen, W., Schmidt, K., 2003. On the use of lipid biomarkers in marine food web analyses: an experimental case study on the Antarctic krill, *Euphausia superba*. Limnol. Oceanogr. 48 (4), 1685–1700.
Syvertsen, E.E., 1991. Ice algae in the Barents Sea: types of assemblages, origin, fate and role in the ice-edge phytoplankton bloom. Polar Res. 10 (1), 277–288.
Taipale, S.J., Kainz, M.J., Brett, M.T., 2011. Diet-switching experiments show rapid accumulation and preferential retention of highly unsaturated fatty acids in *Daphnia*. Oikos 120 (11), 1674–1682.
Tencati, J.R., Geiger, S.R., 1968. Pelagic amphipods of the slope waters of northeast Greenland. J. Fish. Board Can. 25 (8), 1637–1650.
Vader, A., Amundsen, R., Marquardt, M., Bodur, Y. 2021. Chlorophyll *a* and phaeopigments, Nansen Legacy, https://doi.org/10.21335/NMDC-1477580440.

von Quillfeldt, C., 2000. Common diatom species in Arctic spring blooms: their distribution and abundance. Bot. Mar. 43 (6), 499–516.
Wadhams, P., Toberg, N., 2012. Changing characteristics of arctic pressure ridges. Polar Sci. 6 (1), 71–77.
Wang, S.W., Budge, S.M., Gradinger, R.R., Iken, K., Wooller, M.J., 2014. Fatty acid and stable isotope characteristics of sea ice and pelagic particulate organic matter in the Bering Sea: tools for estimating sea ice algal contribution to Arctic food web production. Oecologia 174 (3), 699–712.
Wassmann, P., 2022. The Nansen Legacy: pioneering research beyond the present ice edge of the Arctic Ocean. In: Auad, G., Wiese, F.K. (Eds.), Partnerships in Marine Research: Case Studies, Lessons Learned, and Policy Implications. Elsevier, pp. 33–51.
Wassmann, P., Duarte, C., Agusti, S., Sejr, M., 2011. Footprints of climate change in the Arctic marine ecosystem. Glob. Change Biol. 17 (2), 1235–1249.
Weisshappel, J.B., 2000. Distribution and diversity of the hyperbenthic amphipod family Eusiridae in the different seas around the Greenland-Iceland-Faeroe-Ridge. Sarsia 85 (3), 227–236.
Werner, I., 1997. Grazing of Arctic under-ice amphipods on sea-ice algae. Mar. Ecol. Prog. Ser. 160, 93–99.
Werner, I., 2005. Living conditions, abundance and biomass of under-ice fauna in the Storfjord area (western Barents Sea, Arctic) in late winter (March 2003). Polar Biol. 28, 311–318.
Wickham, H. 2016. ggplot2: elegant graphics for data analysis.
Yunda-Guarin, G., Brown, T.A., Michel, L.N., Saint-Beat, B., Amiraux, R., Nozais, C., Archambault, P., 2020. Reliance of deep-sea benthic macrofauna on ice-derived organic matter highlighted by multiple trophic markers during spring in Baffin Bay, Canadian Arctic. Elem. Sci. Anthr. 8, 047.